NAVAL POSTGRADUATE SCHOOL

Monterey, California

EXPLORATORY DESIGN AND DEVELOPMENT
OF COMPACT NAVAL CONDENSERS

Interim Report #1
Period: 8 Jan - 1 Apr 1979

Investigators:

P. J. Marto, Professor and Chairman
Department of Mechanical Engineering

R. H. Nunn, Associate Professor
Department of Mechanical Engineering

Prepared for: Naval Sea Systems Command, Code 0331

Contract N000247WR9G078

EXPLORATORY DESIGN AND DEVELOPMENT OF COMPACT NAVAL CONDENSERS

Interim Report #1, 8 Jan - 1 Apr 1979

Investigators: P. J. Marto, Professor and Chairman,
Department of Mechancial Engineering
R. H. Nunn, Associate Professor,
Department of Mechanical Engineering

I. BACKGROUND

The objective of the program is to develop a computer-based model for the design and analysis of compact Naval condensers. Both experimental and analytical studies are underway in support of this objective. The experimental program concentrates upon the evaluation of single-tube performance using prototype tubes that have been designed to enhance their performance as heat extraction devices in a condensing medium. The analytical studies have taken two main directions, each dependent upon the other: (1) The development of a comprehensive coding scheme for the calculation of condenser performance in conjunction with modern

design optimization techniques and, (2) the identification and evaluation of reliable (or the best available) theoretical and/or empirical models for the analysis of the thermo-fluid processes that govern the performance of large steam surface condensers.

This report discusses the progress of the analytical portion of the program. The experimental work to date on enhanced tubing is summarized in a forthcoming ASME paper titled "An Experimental Comparison of Enhanced Heat Transfer Condenser Tubing." This paper will be presented at the 18th National Heat Transfer Conference, San Diego, August, 1979. A copy of this paper is enclosed as Appendix A. The experimental work on dropwise condensation has centered around the thesis research of LT. J. Manvel who has tested a variety of tubes designed for the promotion of condensation in the dropwise mode. The results of LT. Manvel's tests will be published in May.

II. OPTIMIZATION

A. CONMIN

The general scheme of optimization to be employed in the investigation is that of CONMIN[1] (Constrained Minimization).

---

[1] National Aeronautics and Space Administration, "CONMIN-A Fortran Program for Constrained Function Minimization," by G.N. Vanderplaats, NASA TM X-62, 2B2, NASA/Ames Research Center, August 1973.

This code has been extensively tested and is well established as a modern and efficient means for the optimization of designs involving several variables and subject to a virtually unlimited number of constraints.

The general optimization problem addressed by CONMIN is as follows:

Find the vector of design variables $\bar{X}$, to minimize the function $F(\bar{X})$ subject to the design constraints

$$G_j(\bar{X}) \leq 0.0 \qquad (j = 1, NCON)$$

$$VLB_i \leq X_i \leq VUB_i \qquad (i = 1, NDV)$$

If a maximum is sought for the objective function, $F(\bar{X})$, one need only minimize its negative. The functions $G_j(\bar{X})$, called "design constraints," are calculable functions of the design variables that are to be held within limits specified by the designer. Examples, in the case of the condenser, include shell-side pressure drop, vapor/gas mixture velocity, shell dimensions, shell-side and tube-side Reynolds numbers, and cooling water pumping power. The second set of constraints are called "side constraints" and limit the feasible range within which the design variables may be adjusted in the search for the optimum. Design variables for the Naval condenser may include such things as tube length, number and pitch of tubes, tube bundle geometry,

cooling water velocity, heat load (steam flow rate), and inside and outside enhancement factors. CONMIN will handle as many as 200 design variables but a more-realistic upper limit is 20. (If a designer is so uncertain about his system that he must allow 20 variables to "float," he should probably put his money into further research.)

The objective function, $F(\bar{X})$, is that property of the system for which an optimum is sought. For the Naval condenser this may be shell volume, for instance. Only one objective function can be specified for a given optimization and its selection is a matter of fundamental importance to the design. A number of tradeoffs arise, not the least of which are those involving uncertainties. Dollar cost, for instance, is a popular objective function but one whose dependency upon the design variables is usually extremely tenuous. Several difficulties of this nature can be addressed by utilizing the optimum sensitivity option of the code. In this mode, the computer can be made to create several optimum designs that differ from each other because of the uncertainty of the values of one or more design variables. In the end, of course, engineering judgement will dictate the choice of designs. The capability to be generated by this study, however, will allow the program manager to compare designs that are each "best" designs subject to each set of known constraints and uncertainties.

CONMIN employs essentially three methods in searching for an optimum. From the initial design furnished by the user, the gradient of the objective function is computed and the first design improvement is in the direction of the negative of this gradient ("steepest descent"). Subsequent iterations in the feasible region (the region that is contained within the constraints) are carried out in accordance with the method of "conjugate directions" which is similar to steepest descent but takes into account the lessons learned in previous iterations. When a constraint is encountered, the determination of the next move towards an optimum must be such that the constraint is not violated. This is accomplished through one of the several schemes known as "methods of feasible directions." The code is extremely versatile and incorporates several innovations for the enhancement of speed and stability.

B. COPES and ANALIZ.

COPES (Control Program for Engineering Synthesis) is a companion calling program for CONMIN. COPES is under development by NASA-Ames (Dr. G. N. Vanderplaats) and the current version has been installed and tested at NPS for use in the present investigation. As shown in Figure 1, COPES directs the computational traffic between the optimizer (CONMIN) and the analysis subroutine (ANALIZ). With COPES, it is possible to treat CONMIN as a "black box." All computational

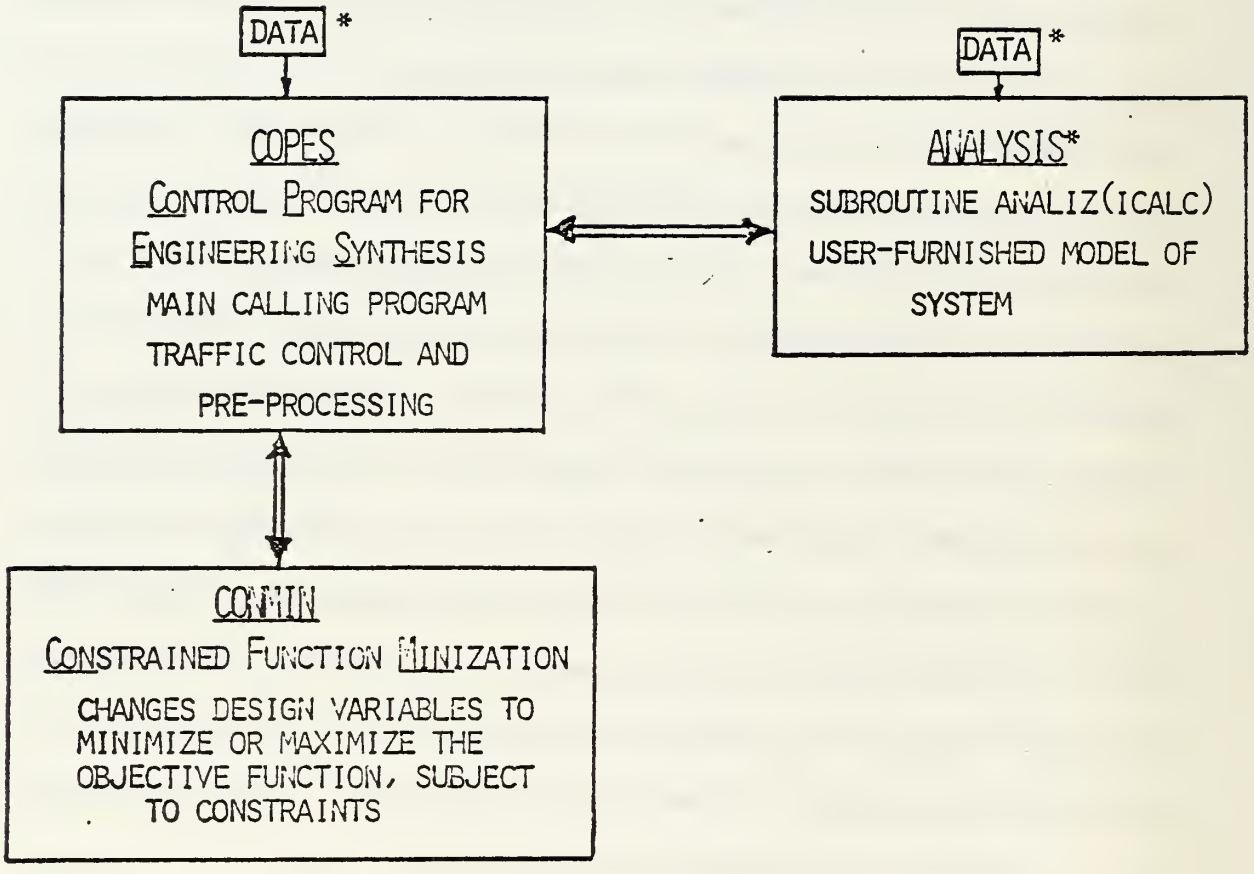

Figure 1. Diagram showing functional relationships between COPES, CONMIN, and ANALIZ.

parameters (step size, convergence bands, etc.) are specified as input data to COPES and when an optimization problem is formulated according to the "rules," the central problem reduces to one of providing the best possible model of the system to be designed. This model is subroutine ANALIZ and its construction constitutes the main goal of the analytical portion of the present study.

During the reporting period, the latest version of the COPES/CONMIN code has been obtained from NASA and installed in the NPS computer system (IBM 360/67). The code is stored in a compiled and linked status on a disk space that is dedicated to the present investigation. Optimization runs have been successfully conducted using an embryonic form of the baseline analysis described in subsequent paragraphs.

III. CODING PHILOSOPHY

During the reporting period a preliminary rationale has been developed for use in formulating an analysis subroutine for naval condensers. A result of this work is the logic flow diagram shown in Figure 2.

In recent years, almost all designers have adopted the use of arrays of heat transfer tubes which are described as bundles. Essentially, each bundle is an operating condenser and in a general computer code it will be necessary to provide means for coupling several bundles together to form a complete main condenser. Each bundle may, in turn, be

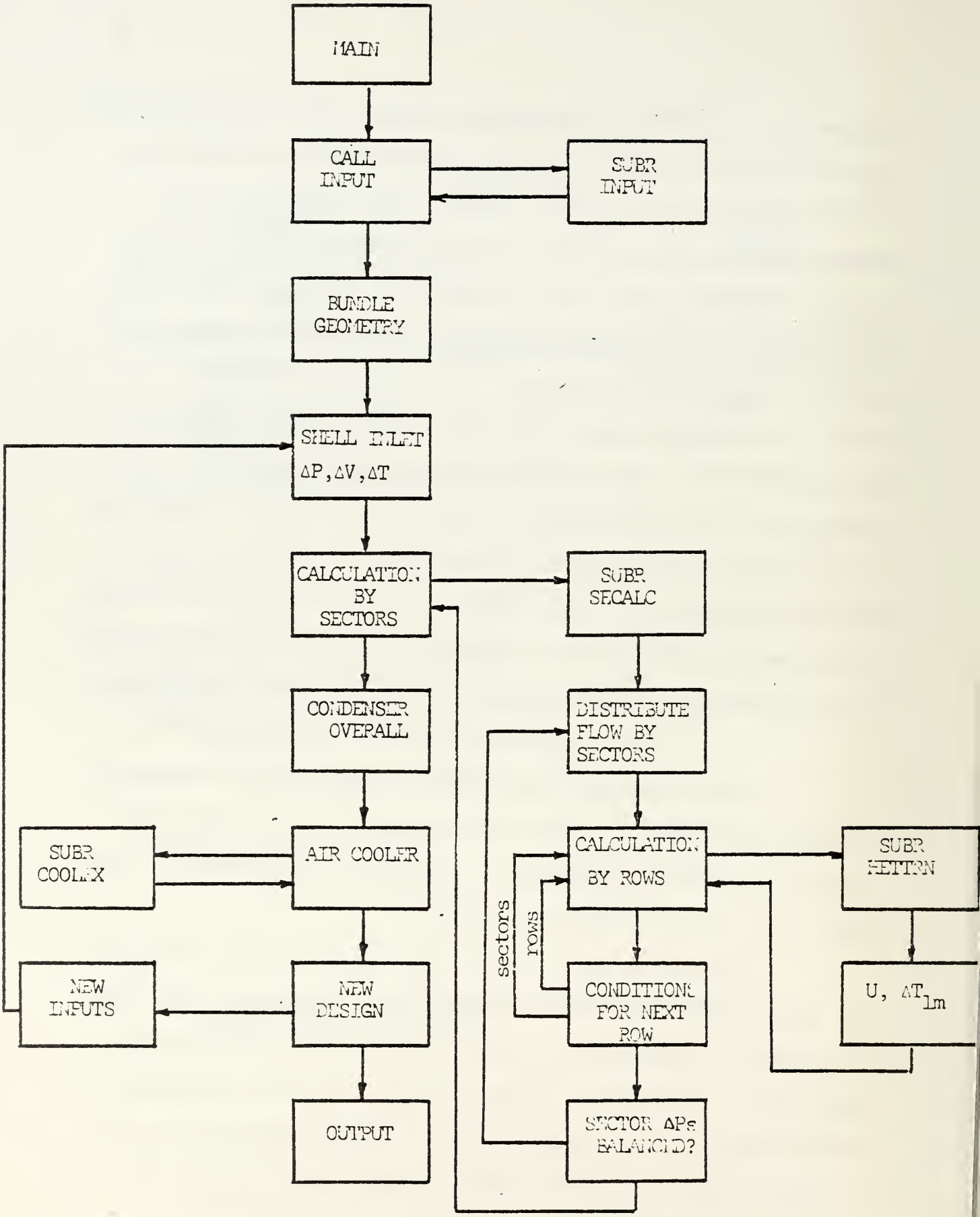

Figure 2. General layout for condenser analysis.

divided into sectors whose coupling will require the matching of the pressure drops through each sector by means of adjusting the fraction of the inlet steam that is apportioned to each. The segmenting of the condenser will improve accuracy when it is necessary to use average properties to calculate bundle performance. In addition, it will be possible to account for condensate take-off between sectors where this is necessary to limit the effects of condensate inundation. The calculation of the performance sector by sector is accomplished in subroutine SECALC in Figure 2.

It is theoretically possible to calculate the performance of each tube, in each row, in each sector, in each bundle. Whether or not this is in fact practical, or even sensible, remains to be seen. In all cases that have been reviewed to date, the performance of large condensers (with 5-10 thousand tubes) is calculated using some sort of "average tube" technique. In any case, the thermal performance of a single (discrete or average) tube is calculated in HETTRN of Figure 2. The heart of the condenser analysis code lies in HETTRN, and it is here that an intensive search is underway to find the best available methods of prediction. The present status of HETTRN is described in section V below.

The hierarchy of calculation in Figure 2 is HETTRN (single tube performance), SECALC (performance of groups of tubes), and MAIN (performance of groups of sectors).

Following the calculations of conditions leaving the main condensing section, the performance of an air cooler section may be calculated, if desired. The simplification in Figure 2 is necessary in order to furnish an overview of the analysis scheme. In HETTRN and in SECALC and perhaps even in MAIN it will be necessary to include iterative loops. In HETTRN, this is mainly because of the dependence of the properties of the vapor, gas, and cooling water upon temperature and pressure, both of which are functions of condensation rate. In SECALC, iteration will be required because of the aforementioned pressure balance requirement. It is easy to imagine further complications, as outlined in Section V of this report.

IV. REVIEW OF EXISTING CODES

Several codes for condenser design are known to exist. The availability of many of these is limited because of proprietary reasons. In any case, however, a comprehensive review is underway to either procure and test existing codes or to learn as much as possible about their ingredients. Although the main effort in this regard is yet to come, some progress has been made during the reporting period. A brief discussion of each area of inquiry is given below:

A. Proprietary Codes

1. Westinghouse. The authors visited the Sunnyvale plant of Westinghouse Electric Corporation and were hosted there by Mr. John Ward. It was learned that there is

an in-house computer-based condenser design capability at Westinghouse but, to-date, only general information is available[1] in the open literature. The code is apparently quite comprehensive, taking into account tube arrangement and density, steam lane design, noncondensible gases, and turbine exhaust nonuniformities. Condensate rain effects are treated but there is no apparent accounting for the effects of vapor shear either separately or in conjunction with condensate rain (the condensate is assumed to drain vertically, regardless of vapor speed or direction). Three-dimensional effects are included by means of "strip-theory" in which tube support plates are taken to be divisions between local two-dimensional flow regions. The Westinghouse code appears to be heavily coupled to data obtained from field tests and should be quite accurate for application to specific existing designs. The general applicability of the code is an area of uncertainty as is the extent to which modern optimization techniques are applied. The authors intend to inquire further into these areas.

2. Heat Transfer and Fluid Flow Service (HTFS). Descriptive material and price quotes have been obtained from

---

[1] E. J. Barsness, "Calculation of the Performance of Surface Condensers by Digital Computer," ASME Paper 63-PNR-2, ASME, New York, 1963.

HTFS. From the available information it is difficult to discern the extent to which the HTFS condenser codes (SCON4 and TASC2) are applicable to the present study. Though aimed primarily at small process condensers, the codes appear to be quite comprehensive. In the input data, for instance, there is an opportunity to call for the accounting of vapor shear effects (but there is also warning regarding the reliability of the results). HTFS has offerred to sell NPS a copy of SCON4 (for £ 1,000) to be used "solely by the Naval Postgraduate School for use by its students." The question of dissemination of knowledge gained from the use of HTFS codes is still an uncertain matter. This issue, as well as the applicability of the HTFS experitse, will be discussed during a visit to the facility planned for late June.

3. Heat Transfer Research Institute (HTRI). The authors accepted the kind invitation of the HTRI management to attend their meeting of the Technical Advisory Committee on February 14-15. Although many useful contacts were made and it was possible to gain a general impression of HTRI capabilities, the meeting did not reveal a great deal concerning the details of the HTRI approach to problems relevant to the present study. The HTRI operation is very much like that of HTFS and there is again the problem of accomodating the proprietary restrictions that may attach to information originating with HTRI. There is, however, a

strong desire in HTRI to cooperate inasmuch as is possible with the NPS study, and a good deal of information has been informally exchanged without difficulty.

The HTRI codes appear to be axtremely comprehensive. As is the case with HTFS, however, it is unlikely that an HTRI program exists for direct use in the present study. It is the internal process modelling schemes that are of most interest to the authors and discussions are continuing along these lines. The HTRI development of flow region maps is especially pertinent to the present study. These maps give criteria for estimating the relative importance of gravity and vapor shear in determining local shell-side film coefficients and (it is believed) the path of condensate rain through the tube bundle. The authors have received some information concerning this area of analysis and a small amount of additional information is available in the open literature. A companion problem is, of course, the modelling of the heat transfer processes when vapor shear effects cannot be neglected.

The services of HTRI have been offered for the validation of codes developed in the NPS study. This would be accomplished by means of case studies in which HTRI would rate condenser designs stemming from the present study. Such a service, if feasible, would be most beneficial and the authors will continue this line of discussion with HTRI.

4. General Atomic Company. Dr. D. Vrable has conducted preliminary condenser design studies in connection

with nuclear plants that use ammonia systems for secondary heat rejection. The computer code developed in conjunction with these studies takes into account enhancement due to treated surfaces and extended surfaces. The heat transfer subroutine of the code uses the correlations of Fujii, et al.[1], which include a Reynolds number (and therefore vapor shear) dependency. (The work of Fujii and his coworkers is especially pertinent to the present study and is under continuing analysis.) Because of the high pressures associated with condensation of ammonia, non-condensible gases are not considered. Vrable includes some cost analysis in his calculations in order to seek an "optimal" design based upon economy of investment. It has been learned, however, that the optimization conducted by Vrable is an informal one rather than the systematic approach to be used in the present study.

B. Codes in the Public Domain

1. HECDOR. The authors have obtained and compiled the HECDOR (Heat Exhanger Cost and Design Optimization Routine)

---

[1] Fujii, T., H. Vehara, K. Kirata, and K. Ota, "Heat Transfer and Flow Resistance in Condensation of Low Pressure Steam Flowing Through Tube Banks," J. Heat and Mass Transfer, 15, 247-260, 1972.

code developed under DoE auspices at EG&G Idaho, Inc. The usefullness of the HECDOR code in the present study is extremely limited because of the rather oversimplified approach to the thermal performance of a condenser (constant properties and minimal tube-tube interaction, among other things). The virtue of HECDOR appears to lie in the optimization method in which a Lagrange multiplier technique is used to obtain implicit analytical expressions for optimum conditions. In addition, since the objective function is cost, there is a considerable amount of information provided that may prove useful in developing an approach to the cost analysis of naval condensers.

2. Heat Exchange Institute (HEI). The HEI design methods are noteworthy for their simplicity. In the present study, simplicity, though virtuous, is no longer a necessity. The problems associated with the HEI method (insensitive to shell-side processes, not amenable to the inclusion of enhancement effects, etc.) have been described by Johnson[1] and are such as to preclude its use in the present study, except, perhaps, as a rough-cut backup. The authors do plan to consult further with HEI researchers in order to determine their views as to the most reliable means for more-detailed calculations.

---

[1]Johnson, C. M., "Marine Steam Condenser Design Using Numerical Optimization," MS. Thesis, NPS, Monterey, CA., Dec. 1977.

3. ORCON. This code, developed at the Oak Ridge National Laboratory, is by far the most comprehensive code for condenser performance that has been found to be available to the public. The circular-bundle version of ORCON forms the analysis subroutine used by Johnson[1] in his studies. In the present study, the version of ORCON for use with rectangular tube bundles has been compiled and debugged and has served as the main source of computer-derived results during the reporting period. Use of the rectangular bundle version of ORCON, rather than the circular bundle version, eliminates a few of the uncertainties associated with the calculation of the effects of condensate rain and the simpler tube-tube geometry allows an easier interpretation of computed results. As a result of the extensive use of ORCON during the reporting period, the internal workings and overall philosophy of codes of this nature (which is largely that of Fig. 1) are now well-understood. Some of the features and limitations of ORCON are summarized below:

a. ORCON allows the calculation of either vertical or horizontal flow of steam/gas mixture across horizontal cooling tubes. There is no provision for flow

---

[1] Johnson, C. M., "Marine Steam Condenser Design Using Numerical Optimization," MS. Thesis, NPS, Monterey, CA., Dec. 1977.

at intermediate angles except for the calculation of radial flow in the circular bundle version.

b. There is a means for correcting the condensate film coefficient for the effects of rain. The method is based upon Eissenberg's[1] adaptations to the classical method of Nusselt. The correction only accounts for the distribution of condensate rain upon lower tubes in a gravity-dominated flow and does nothing else to modify the classic Nusselt model for laminar film condensation on an isolated tube.

c. Non-condensible gases (up to four species) are taken into account by the use of the Reynolds flux model, as elaborated by Spalding, and an empirical correlation suggested by Eissenberg. The method appears to be similar to that employed by HTFS and represents the state-of-the-art in this rather uncertain area.

---

[1]Eissenberg, D. M., "An Investigation of the Variables Affecting Steam Condensation on the Outside of a Horizontal Tube Bundle," Ph.D. Thesis, V. Tennessee, Dec. 1972.

d. ORCON is easily modified to include enhancement of the inner and/or outer film coefficients. If necessary, the enhancement may be calculated as a function of local conditions within the condenser.

e. ORCON, as in all other known cases, includes fouling effects only as a constant resistance term.

f. All fluid properties are continuously variable and change with pressure and temperature throughout the condenser. The latter quantities are allowed to vary due to inlet, outlet, and tube-tube flow variations, as well as viscous losses, and the effects of condensation.

g. Bundles can be segmented into as many as four sectors in the case of horizontal flow (one sector only for vertical flow.). Condensate removal is not provided for but could be easily incorporated between sectors.

h. The overall heat transfer coefficient is calculated on the basis of an "average" tube in each row of tubes. This is a basic limitation of the code that is

somewhat relieved by the ability to calculate performance by sectors.

i. Vapor shear effects are not included. There is some capability to simulate these effects by weighting the distribution of condensate rain in the direction of flow, but this method is not founded upon any quantitative physical model.

j. ORCON calculations are based upon two-dimensional flow assumptions. However, the program organization appears to be ameanable to the expansions and revisions that would be necessary if a three-dimensional analysis were to be developed.

Some minor alterations to ORCON have been instituted in order to adapt the code to suit the needs of the present study. These alterations consist, in the main, of the creation of several subroutines within the heat transfer subroutine (HETTRN) in accordance with the thermal resistance method of analysis. At the present time, there are four special subroutines for the calculation of internal convective resistance, the condensate film resistance, the effective film resistance due to non-condensible gases, and corrective functions for the effects of condensate rain. In this form, it will be possible to use the code to measure the differences in condenser performance due to variations in the analysis models. Other subroutines may be added as it becomes necessary to take additional effects into account. Extensions of this nature might include corrections for vapor shear and the calculation of variable

enhancement and/or fouling factors.

The ORCON methodology, in its present form, appears to be conservative. That is, the condenser performance predicted by the code is consistently less than that expected from experience. This conservative nature is illustrated in Fig. 3 in which the results of several condenser performance calculations are summarized. The test case is the full power load for the main condenser of the USS Kennedy (CVA-67). Input specifications include 400,000 lb/hr of saturated steam and 45 lb/hr of entrained air flowing horizontally across 6,612 tubes arranged in two main bundles that are symmetrical about a central steam lane. The measure of performance used in Fig. 3 is the exit fraction (EXITFR) of steam vapor leaving the condenser as a percentage of that which enters.

In Fig. 3a the effects of variation in the condensate rain model are shown. The abcissa here is the number of sectors into which each bundle is divided for calculation purposes. It is seen that for the condenser aspect ratio (height/width) of 0.6 used in Fig. 3a, the complete removal of rain effects results in a "best" condition of about 24% exit fraction. (This no-rain result is, incidentally, independent of the numbers of sectors used in the calculation.) Figure 3b shows the effects of increasing aspect ratio with and without condensate rain (the various models for rain effects are discussed in the following section). Large

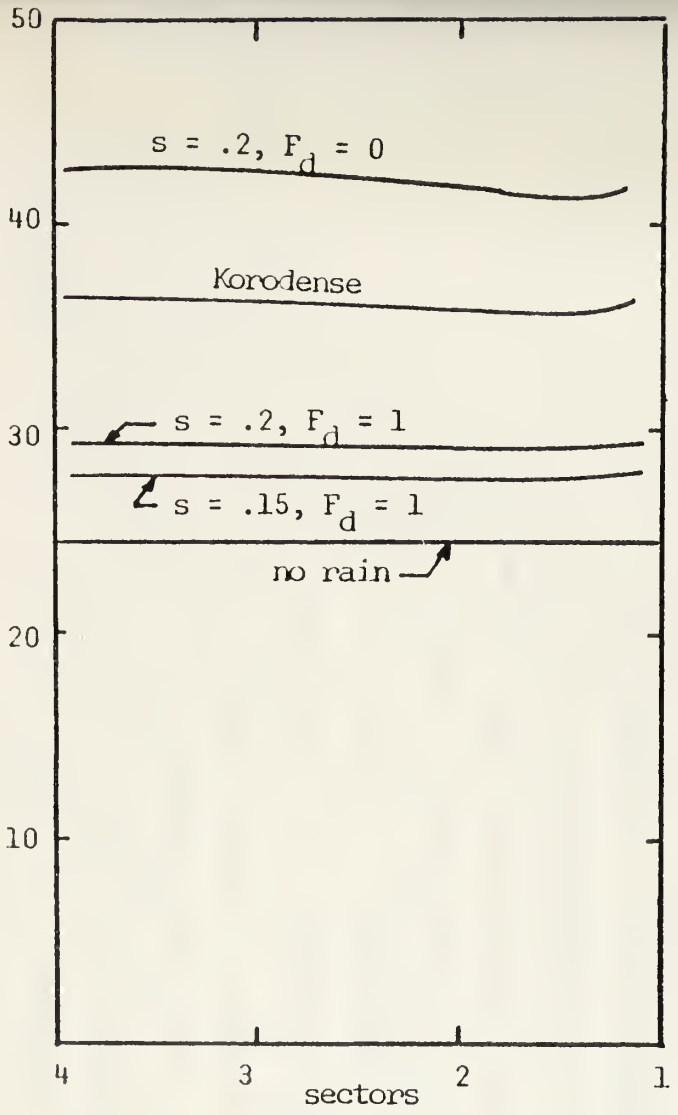

a. Effect of sectoring, h/w = 0.6

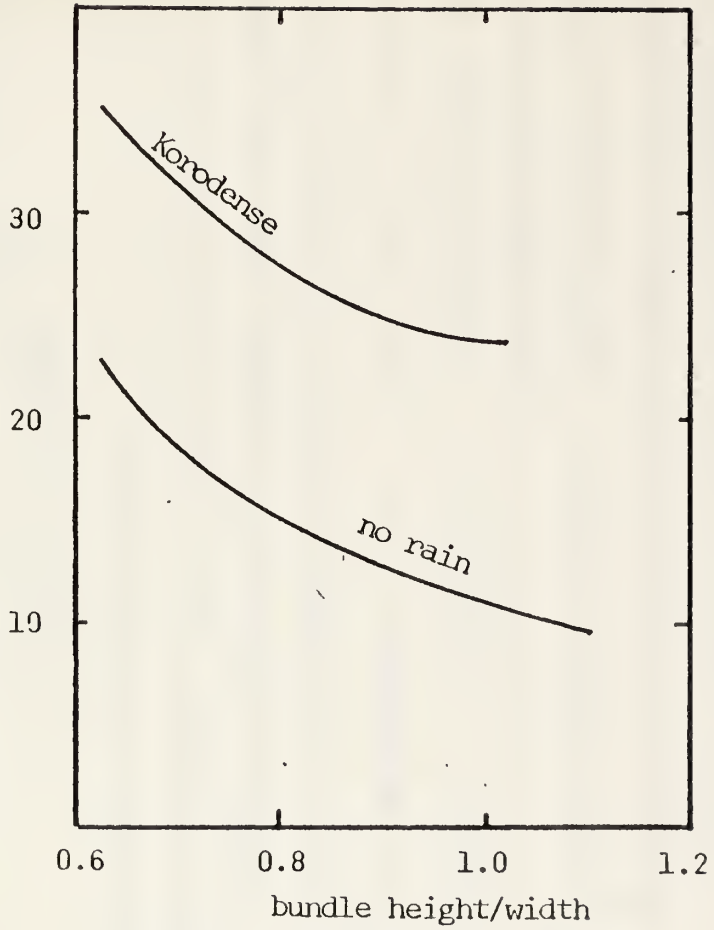

b. Effect of bundle aspect ratio

Figure 3. ORCOM predictions of performance of CVA-67 main condenser.

values of the aspect ratio correspond to large numbers of tubes in relatively few vertical rows exposed to the horizontal flow of the vapor/gas mixture. The improvement in performance with increasing aspect ratio is apparent, but an aspect ratio of 1.0 is near the upper limit of realism for simulation of the CVA-67.

Figure 3 is presented here to illustrate the conservative nature of the predictive model as it now stands. The problems associated with those and other calculations are discussed in the following section.

V. SPECIAL PROBLEMS

The issues discussed in this section are termed "special" in that they are deemed to be pertinent to the prediction of condenser performance while, at the same time, they are encumbered by relatively large uncertainties in the present state-of-the-art. In large Naval surface condensers the two-phase processes occur on the shell side of the tube arrays. Thus, it is not surprising to find that the central area of concern is with this side of the condenser heat-exchange system and all of the special problems discussed below are related to this region. Inside the cooling tubes, the seawater flow is assumed to be turbulent and fully-developed; a situation which has received ample theoretical and experimental treatment in the heat-transfer literature. In other words, the prediction of the thermo-fluid effects on the tube side of Naval condensers is a relatively precise art, with the exception of fouling resistance.

The problems discussed below represent those that have assumed a status of significance during the reporting period. They are coupled processes and their listing in this fashion should not imply otherwise.

A. Condensate Rain. In Appendix B, it is shown that the classical Nusselt theory, which assumes that all condensate drains directly to the tube directly below, leads to an expectation that the condensate film coefficient, h_n, for the nth tube in a vertical row of tubes, should be related to the film coefficient for a single tube, h_N, by the form

$$\frac{h_n}{h_N} = n^{(1 - s)} - (n - 1)^{(1 - s)}$$

where s may vary from 0.07 to 0.20 according to experimental results and s = 0.25 according to the theory due to Nusselt. The extent to which this ratio is less than one is a measure of the degree of degredation of the performance of the n-th tube due to the (n - 1) tubes above it. If one asks the question, "How many tubes must drain from above to reduce the value of the condensate film coefficient on the local tube to 50% of its single-tube value?", one finds that with h_n/h_N = 0.5 the resulting value of n may range from about 5 to more than 1000 within the range given above for s. Clearly the Nusselt theory is too conservative and the extent of the discrepancy can be several orders of magnitude. The simple theory shown above and developed in Appendix B cannot be sufficient.

Eissenberg (see Appendix B) has improved the situation by providing an alteration to the theory to account for the spacing and orientation of the tubes relative to each other. Tubes vertically aligned and close together are more affected by rain from above than is the case for tubes that are staggered arrays and far apart. The Eissenberg model does not, however, depart from the basic Nusselt assumptions of gravity-dominated laminar condensate films, and cannot be expected to give valid results for the high shell-side Reynolds numbers and heat fluxes present in large Naval condensers.

It has become apparent to the authors that an improved model for the shell-side condensate film coefficient must be obtained in order to account for the effect of high vapor velocities upon condensate rain and to provide a rationale for incorporation of these effects into models of the local and overall performance of condensing tubes in bundles.

B. Noncondensible Gases. Appendix C outlines the method used in ORCON to determine h_{eff}, the conductance of the hypothetical film of gas superimposed upon the condensate film. Initial runs with ORCON indicate that when noncondensible gases are held to concentration levels of less than about 10 ppm by weight it is unlikely that their effective film resistance will affect overall condenser performance by more than 1%. A more subtle effect of the presence of non-condensible gases on the shell side is the modification of

mixture properties and the subsequent alteration of an already-complex two-phase flow problem. The transport and heating of condensate droplets as they progress, through a condenser bundle may depend upon the presence of noncondensibles in a way that is as-yet undetermined.

C. Vapor Shear. The velocity (Reynolds number) of the condensing medium has been found to be an important factor in the performance of condensers. In low-speed flows the trajectory of condensate droplets is governed by the influence of gravity. At higher speeds the trajectories are significantly modified and, in fact, the droplets themselves can be shattered to the point that the condensate flow is in the form of a mist rather than discrete droplets. In addition, the speed and direction of the vapor/gas mixture can influence the condensing performance of a single tube by shear effects at the vapor/condensate interface and, ultimately, the stimulation of turbulent flow in the condensate film and stripping of the film from the tube surface.

Many of these problems have been addressed in the open literature but several of the most advanced techniques appear to be of a proprietary nature. Appendix D presents a simple model that allows the estimation of the conditions governing the relative dominance of gravity and shear from the point of view of droplet trajectory. Analyses such as these will be expanded to incorporate information gained from the continuing search for the best available modelling methods. Vapor

velocity effects and their coupling with condensate rain processes are thought to be the chief source of conservation in ORCON and this area of investigation has been assigned as the research topic for the Engineer's thesis of Lt. H. M. Holland.

D. Bundle Pressure Drop. Pressure changes occur on the shell side of the condenser bundles for three main reasons:

1. Reversible losses or gains in kinetic heads due to change in flow cross-sections.
2. Dissipative processes due to viscous effects.
3. Condensate removal which lowers the steam partial pressure which, in turn, reduces the equilibrium temperature of the mixture as it flows through the bundle.

The overall pressure drop together with the air extraction system, determines the back-pressure against which the turbine must exhaust. In addition, the local pressure at each point in the condenser will influence the mixture properties at that point and, directly and indirectly, the local heat removal rate. Finally, the existence of pressure gradients in the condenser influences the nature and direction of the flow in both a local and a global way.

All of the problems previously mentioned are dependent upon and influence the condenser pressure distribution. The problem is one of two-phase multi-component flow with highly coupled variables. As such, it is a matter of current

research and one which will require careful consideration in the formulation of the optimal design code.

E. Validation of the Models. At present, the CVA-67 full-power operating point is being used as a baseline for comparison. Even this point is poorly documented (what is the actual exit fraction for CVA-67 at full power?) and as refinements to the code continue, it will become increasingly important to have a reliable set of operating condenser data.

VI. SUMMARY AND FUTURE PLANS

During the reporting period, two main computer codes have been developed. The baseline code is to serve as the foundation for the construction of the final code. In its present form, this program consists simply of a single row of tubes in horizontal steam flow, and only inside convection and shell side condensate film resistances are incorporated. The baseline code has been coupled to the optimization code (COPES/CONMIN) and has been successfully tested in the optimization mode. The second code is the modified ORCON program which is serving as a test platform for various candidate models of the complex processes occurring in large condenser tube bundles.

Tests with the existing codes have indicated several areas where improved semi-empirical predictive methods must be developed. These indications are supported by the information gained from discussions with researches who are active in the relevant fields. The main immediate goal in

the present study will be to continue these discussions with a view towards further defining the best methods presently available.

Within the following reporting period, the authors will make several trips to US industrial and government facilities. In addition, an itinerary has been developed for personal contact with appropriate individuals and agencies overseas. The consultation activities of the authors, past, present, and future, are documented in Appendix E.

APPENDIX A

AN EXPERIMENTAL COMPARISON OF ENHANCED HEAT TRANSFER CONDENSER TUBING

P. J. Marto
Professor
Member ASME

LT. D. J. Reilly, USN
Graduate Student

LT. J. H. Fenner, USN
Graduate Student

Department of Mechancial Engineering
Naval Postgraduate School
Monterey, California 93940

ABSTRACT

Eleven corrugated tubes were tested to compare their heat transfer and pressure drop characteristics to a smooth tube. Steam was condensed on the outside surface of each test tube, which was mounted horizontally in the center of a dummy tube bundle, and cooled by distilled water. A corrected overall heat transfer coefficient was determined by subtracting the wall resistance from the measured overall resistance. The inside and outside heat transfer coefficients were determined using the Wilson plot technique.

Corrected overall heat transfer coefficients were as much as twice those of the smooth tube, while cooling water pressure drop was as much as ten times the smooth tube. Most of the heat transfer improvement occurred on the water-side, with little increase, or in some cases a decrease, on the steam-side. The data show that pitch or helix angle, as well as groove depth, are important variables in enhancing heat transfer.

NOMENCLATURE

A_n	Nominal surface area of test tube (m^2)
C_i	Sieder-Tate coefficient
c_p	Specific heat (kJ/kg C)
D_i	Inside diameter (m)
D_o	Outside diameter (m)
e	Tube groove depth (mm)
f	Fanning friction factor
G	Flow rate per unit area ($kg/m^2 sec$)
g	Acceleration of gravity (m/sec^2)
g_c	Gravitational constant ($kg\ m/N\ sec^2$)
h	Heat transfer coefficient (W/m^2 C)
h_{fg}	Latent heat of vaporization (W sec/kg)
k	Thermal conductivity (W/mC)
L	Length of test tube (m)
$\dot{m}$	Mass flow rate of cooling water (kg/sec)
Nu	Nusselt number = hD/k
p	Tube spiral pitch (mm)
ΔP_c	Corrected Pressure drop across test section (kPa)
Pr	Prandtl number = $\mu c_p/k$
R_w	Thermal resistance of tube wall (m^2C/W)
Re	Reynolds number = DG/u
Tc	Temperature of cooling water (C)
Tv	Temperature of vapor space (C)
U_c	Corrected overall heat transfer coefficient (W/m^2C)
U_n	Overall heat transfer coefficient (W/m^2C)
μ	Dynamic viscosity (kg/m hr)
ρ	Fluid density (kg/m^3)

Subscripts

a	Augmented
b	Fluid at the bulk temperature in C
f	Film
i	Inside, or inlet
n	Nominal
o	Outside, or outlet
s	Smooth, or saturation
v	Vapor
w	Wall

INTRODUCTION

In recent years, there has been an increased awareness regarding the use of enhanced heat transfer surfaces in the design of heat exchangers. Bergles [1-4] has summarized extensive works in both single phase and two phase heat transfer enhancement and has compared the results of different experimenters using several performance criteria [5, 6].

A variety of studies has been conducted pertaining to condenser applications. Palen, Cham and Taborek [7, 8] condensed steam on enhanced tubes in a horizontal tube bundle configuration containing 196 tubes, and compared results to similar smooth tube tests. The outside diameter of the tubes was 25.4 mm, and shell-side steam pressure was maintained at either 480 kPa or 825 kPa absolute. Young, Withers and Lampert [9] conducted bundle comparison tests of smooth and enhanced tubes with outside diameters of 15.9 mm and 25.4 mm. Steam pressure was kept at 6.9 kPa or 101.4 kPa absolute and cooling water velocity through each tube was varied from about 0.91 m/sec to 1.98 m/sec. Catchpole and Drew [10] conducted tests on five different 15.9 mm OD, grooved tubes in both a single-tube and bundle configuration. Steam was supplied at 13.79 kPa and the cooling water velocity through the tubes was maintained at 3.05 m/sec. Cunningham and Milne [11] studied the effect of helix angle on the performance of horizontal roped tubes. Steam was supplied at atmospheric pressure, and cooling water velocity was varied up to 4 m/sec. The tubes were approximately 12.5 mm in outside diameter, and were tested in a single-tube configuration. Newson and Hodgson [12] condensed steam at atmospheric pressure on a variety of enhanced tubes in a vertical orientation. Similar tests were conducted by Combs [13] for ammonia, and by Combs, Mailen and Murphy [14] for different refrigerants.

The above-mentioned investigations have been conducted under widely varying test procedures and physical environments, leading to difficulty in attempting to compare results. The purpose of this work is therefore to obtain heat transfer and pressure drop data of a variety of spirally fluted condenser tubes, and to compare their performance to smooth tube operation using a single apparatus under identical operating conditions.

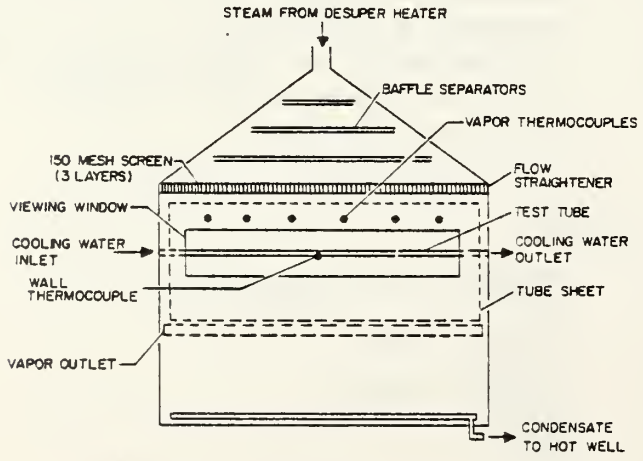

Fig 1. Schematic Front View of Test Condenser

EXPERIMENTAL APPARATUS

The condenser apparatus used during these tests is shown schematically in Figures 1 and 2, and is described in more detail by Beck [15], Pence [16] and Fenner [17]. The test condenser is made of stainless steel. Steam from an electrically fired boiler enters from the top at 20.7 kPa, after passing through a desuperheater to keep the superheat less than 10C. It then expands into the test section, and is uniformly distributed by baffle separators, three layers of 150 mesh screen, and a flow straightener. The steam is guided through a horizontal tube bundle with a spacing to diameter ratio of 1.5. As shown in Figure 2, glass windows exist on each side of the condenser to view

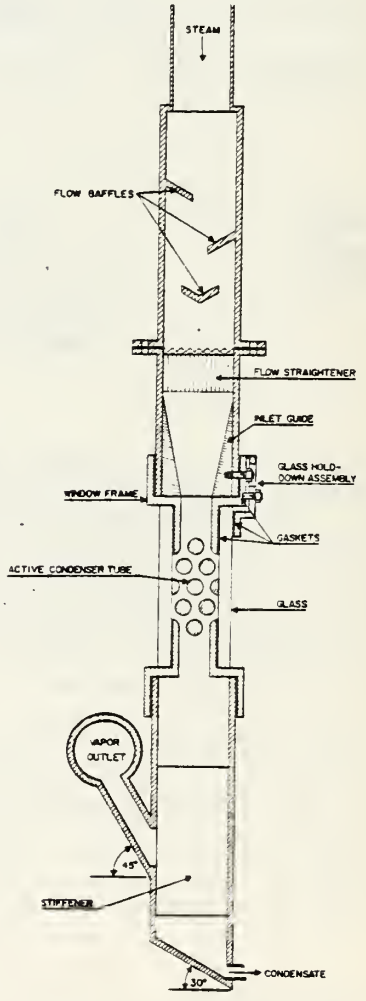

Fig. 2. Schematic Side View of Test Condenser

the condensation process. Only the center tube within the bundle is active, with cooling water flowing through it. The other dummy tubes are provided to simulate actual steam flow conditions in a large tube bundle. The steam which is not condensed on the test tube flows through the outlet manifold to a secondary condenser. The condensate is collected at the bottom of the condenser and flows to a hotwell where it is pumped back to a feed-water heater prior to re-entering the boiler. All test section components are insulated with foam rubber insulation.

Cooling water is pumped from a supply tank to the test tube via one of two calibrated rotameters using galvanized piping with an inside diameter of 26.6 mm. The water returns to the supply tank via a dry cooling tower as shown in Figure 3. The piping inside diameter is reduced to 13.4 mm approximately 0.76 m ahead of the test tube to insure fully developed flow at its entrance. Pressure taps are installed in the permanent piping at the ends of the test tube to permit the measurement of the overall pressure drop. All cooling water lines are insulated with 25 mm thick foam rubber.

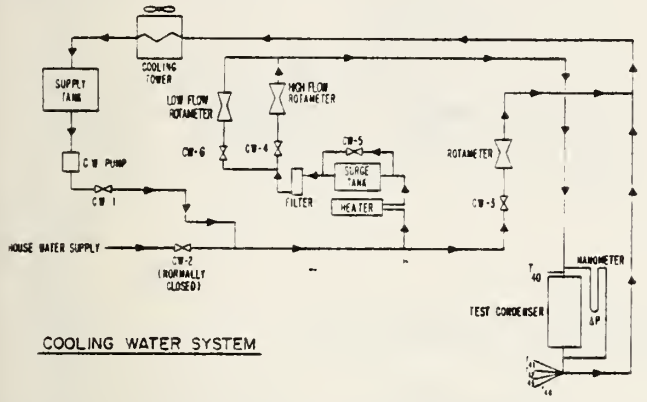

Fig. 3. Schematic Diagram of Cooling Water System

The test condenser pressure is measured with an absolute pressure transducer as well as with a mercury manometer. Cooling water pressure drop across the test tube is measured with a mercury manometer. Stainless steel sheathed, copper-constantan thermocouples, calibrated to an accuracy of ± 0.1C, are used to measure the vapor space temperature, the inlet and outlet cooling water temperature, and the test tube wall temperature.

Test Tubes

Eleven different enhanced tubes, with nine different geometries, were tested and compared to a smooth tube. The enhanced tubes were obtained from several manufacturers. Each tube had a nominal outside diameter of 15.9 mm. They had a 0.91 m long, central enhanced section with a 0.155 m long smooth section at each end, giving an overall length of 1.22 m. All of the enhanced tubes were spiraled along their active lengths, although the method of spiral development varied considerably with manufacturer. Figure 4 is a photograph showing eight of the spiraled tubes. Table 1 lists the detailed characteristics of the tubes.

TEST PROCEDURES

Prior to any run, each condenser tube was lightly brushed and treated chemically to insure good wettability of water on its surface [16, 18, 19]. After placing a test tube in the condenser, and establishing cooling water flow through it, steam flow was gradually increased to the test section giving an operating pressure near 20 kPa absolute. This resulted in a steam velocity over the tubes of approximately 8 m/sec. Steady state conditions were reached approximately one hour from the time steam flow was introduced into the condenser.

For each data point obtained, the cooling water velocity through the active tube was fixed at a prescribed value between 1 to 8 m/sec. At steady state conditions, the following data were recorded:

vapor temperature,
tube wall temperature,
cooling water inlet and outlet temperature,
cooling water pressure drop, and
cooling water flow rate.

Table 1. Enhanced Tubing Characteristics

Tube No.	Run No.	Material	Thermal Conductivity (W/m°C)	Inside Diameter (mm) D_i	Outside Diameter (mm) D_o	No. of Groove Starts N	Helix* Angle (Deg)	Groove** Depth (mm) e	Pitch*** (mm) p	p/D_o	e/D_o	Area Ratio (A_o/A_n)
GA-1	2	Aluminum (6061)	237.1	13.46	16.00	13	30	1.4	64.0	4.0	0.09	1.18
GA-2	1	Aluminum (6061)	237.1	13.31	16.00	10	45	1.4	33.5	2.09	0.09	1.12
GA-3	3	Aluminum (6061)	237.1	13.46	16.00	7	60	1.4	20.0	1.25	0.09	1.02
K-1	9	90-10 Copper-Nickel	44.7	13.39	15.88	1	65	0.36	9.81	0.62	0.022	1.0
K-2	12	90-10 Copper-Nickel	44.7	13.39	15.88	1	70	0.51	9.64	0.61	0.032	1.0
K-3	13	Aluminum (3003)	172.8	13.39	15.88	1	64	0.41	9.67	0.61	0.026	1.0
K-4	11	Aluminum (3003)	172.8	13.39	15.88	1	74	0.58	9.58	0.60	0.031	1.0
K-5	14	Titanium	17.0	14.48	15.88	1	75	0.61	5.97	0.38	0.038	1.0
T-1	4	Copper (Alloy 122)	339.2	14.45	15.88	3	30	2.67	50.43	3.18	0.168	1.07
T-2	5	Copper (Alloy 122)	339.2	14.45	15.88	3	45	3.25	36.78	2.32	0.205	1.20
T-3	6, 17	Copper (Alloy 122)	339.2	14.45	15.88	3	60	3.35	22.58	1.42	0.211	1.46

*Helix Angle = Angle measured from tube axis to flute axis.
**Groove Depth = distance between the ridge and the trough of a corrugation as measured on the outside of the tube.
***Pitch = distance required along the tube for a given groove to rotate through 360°.

Fig. 4. Photographs Showing the Geometries of the Enhanced Tubes

From this data, the overall heat transfer coefficient was calculated using a nominal surface area of a 16 mm OD smooth tube:

$$U_n = \frac{\dot{m} c_p}{A_n} \ln \left(\frac{T_v - Tc_i}{T_v - Tc_o} \right) . \quad (1)$$

A corrected overall coefficient was then obtained by subtracting a calculated wall resistance from the overall measured thermal resistance:

$$U_c = \frac{1}{\frac{1}{U_n} - R_w} . \quad (2)$$

Values of the calculated wall resistances were estimated for each of the enhanced tubes by using the thermal conductivity values listed in Table 1 along with approximate wall thickness values. The exact wall resistance of fluted tubes is very difficult to calculate due to the complicated geometry and the non-uniform heat transfer rates which occur between the bottom and the top of the grooves. Fortunately, during these tests, the wall resistance was not significant, and it was estimated that, in general, a 50 percent uncertainty in wall resistance would cause less than a 10 percent uncertainty in U_c. The inside and outside heat transfer coefficients were calculated following the well-known Wilson plot technique [17, 18, 20, 21].

In order to find the friction factor for each of the enhanced tubes, the overall cooling water pressure drop was corrected for the smooth ends as well as for the expansion and contraction effects which occur at the exit from and entrance to the enhanced portion of the tubes [17, 18]. This corrected pressure drop ΔP_c was then used to define a Fanning friction factor:

$$f = \frac{\rho \, \Delta P_c \, g_c}{2(L/D_i)G^2} . \quad (3)$$

The rotameters used in this experiment were calibrated using a stopwatch and a scale. All thermocouples were calibrated against a platinum resistance thermometer in a silicone oil bath. Uncertainties in these measured values led to uncertainties in the calculated quantities mentioned above. The details of these uncertainty calculations are presented by Fenner [17] and Reilly [18]. Some typical uncertainties are listed below:

U_n: ± 6%
h_i: ± 10%
h_o: ± 15%
f: ± 3%
C_i: ± 8%

RESULTS AND DISCUSSION

Heat Transfer Coefficients

Figures 5, 6, and 7 show the corrected overall heat transfer coefficient versus cooling water mass flow rate for each of the corrugated tubes. As

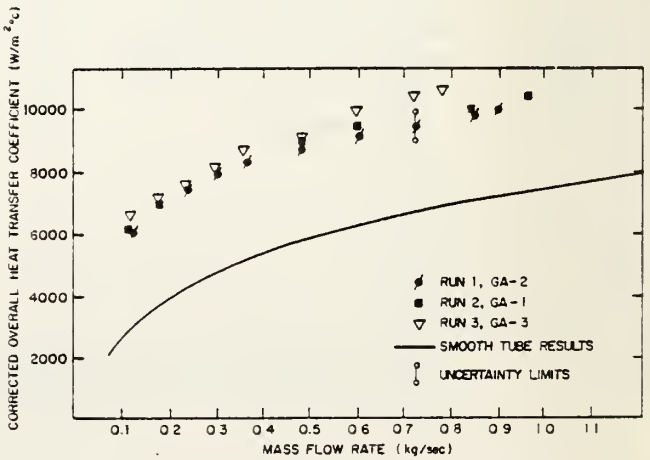

Fig. 5. Corrected Overall Heat Transfer Coefficient for the Type GA Tubes

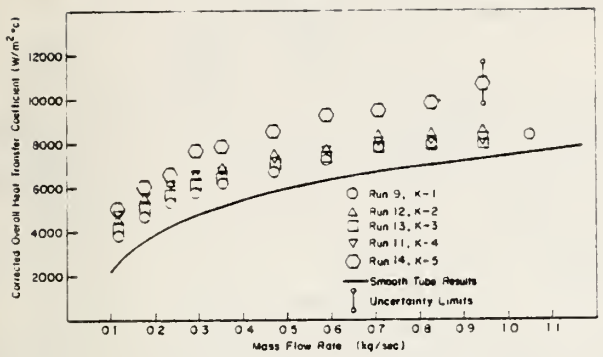

Fig. 6. Corrected Overall Heat Transfer Coefficient for the Type K Tubes

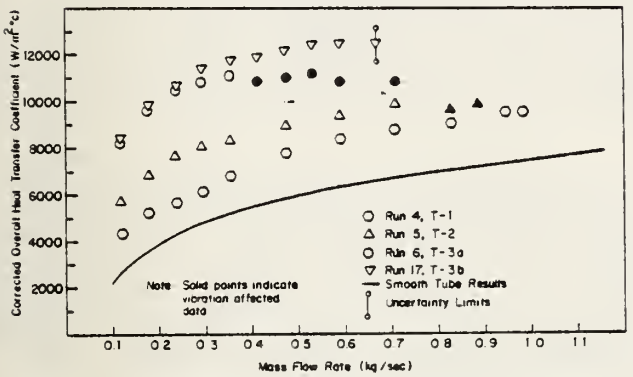

Fig. 7. Corrected Overall Heat Transfer Coefficient for the Type T Tubes

expected, the heat transfer performance of these tubes is clearly superior to the smooth tube. For example, at a cooling water mass flow rate of 0.5 kg/sec, corresponding to a velocity of 3.6 m/sec, and a Reynolds number of 55,000 inside the tube, the corrugated tubes show an increase in the corrected overall coefficient of from 16% to 100% over the smooth tube value. The tubes K-1 through K-5 show the smallest increase over the smooth tube (from 16 to 42 percent) due to their rather shallow groove depth, as seen in Figure 4, and as listed in Table 1. Tubes GA-1 through GA-3 perform better, showing an increase of 51 percent for GA-2, 56 percent for GA-1 and 62 percent for GA-3 at the same cooling water mass flow rate of 0.5 kg/sec. This improved performance is due to the numerous, deep grooves in this tube as shown in Table 1. The best overall performance is exhibited by tube T-3 which shows an increase of 104 percent. When comparing this tube to the others tested, it is seen in Table 1 that it possesses the most severe groove depth of any of the tubes, reaching 20 percent of the tube outer diameter. This gives the largest surface area ratio of 1.46 as well.

Effect of Tube Vibration

Of interest in Figure 7 is the effect of vibration on tube performance, as indicated by the solid data points. Tube T-2 was observed to vibrate visually and audibly at its maximum cooling water flow rates, and tube T-3 was observed to vibrate at much lower cooling water flow rates. These tubes, especially T-3, had low lateral strength. Movies were therefore made with varying cooling water flow rates through tube T-3 to observe the initiation of tube vibration. This was done both with and without steam condensing on the tube. Copies of the 16 mm movie film showing the vibration phenomena, both with and without condensation taking place, are available on request.

Vibration was observed to begin visually at a cooling water velocity of about 1 m/sec when steam was not supplied to the condenser. This indicated that this phenomena was not caused by vortex shedding on the outside, but by cooling water turbulence on the inside. With steam supplied, however, vibration was not visually dectectable until velocities of about 3 m/sec were reached. This was felt to be due to the damping effect of the added mass of the condensate flooding the tube grooves. Audible evidence of the vibration was heard both with and without steam supplied to the condenser at cooling water velocities of about 1.8 m/sec and above.

It was decided to run tube T-3 with additional supports to see if the vibration could be controlled, and to observe the effect on tube performance. Therefore, for Run 17, the active length of the tube was supported against the adjacent tubes using two circular ring braces equally spaced along the tube axis such that the active length was reduced to three equal lengths of approximately 1/3 meter each. During this Run no vibration was observed either visually or audibly.

Figure 8 illustrates this vibration phenomena. As a note of clarification, the reader may wish to refer to Figure 2 while studying Figure 8. The

(a) Cooling Water Velocity is 3 m/sec

(b) Cooling Water Velocity is 4 m/sec

Fig. 8. Photographs Showing Effect of Tube Vibration on Condensate Ripples, Tube T-3

pictures are views upward between the smooth dummy half-tube and the smooth dummy whole-tube below it, such that the bottom of the enhanced tube can be seen just below the smooth dummy half-tube. Figure 8(a) shows condensation on tube T-3a which was unsupported. The cooling water velocity is 3 m/sec, and no vibration is evident. Figure 8(b) shows a view of the same tube

with a higher cooling water velocity of 4 m/sec while vibration is occurring. The light reflections off the surface of the condensate in the figure are due to surface ripples on the condensate from the vibration.

The effect of this vibration on heat transfer is clearly seen in Figure 7. By comparing tubes T-3a, Run 6 (unsupported) and T-3b, Run 17 (supported), it is clear that there is a significant improvement in the corrected overall heat transfer coefficient when the vibrations do not occur. As indicated earlier in the photographs, these tube vibrations cause the condensate to have surface waves which may hold up the condensate drainage off the exterior of the tube, thickening the condensate film. By adding the additional tube supports, and preventing vibration, the drainage was improved, leading to higher outside heat transfer coefficients.

Inside and Outside Coefficients

Using the Wilson plot technique, the inside and outside heat transfer coefficients were calculated. The inside heat transfer coefficient was assumed to follow the Sieder-Tate relationship [22]:

$$Nu = \frac{h_i D_i}{k_b} = C_i Re^{0.8} Pr^{1/3} (u/u_w)^{0.14}, \qquad (4)$$

and C_i for the smooth tube was measured as 0.025. This compares favorably with the normally quoted value of 0.027 [22]. The outside heat transfer coefficient was assumed to follow the Nusselt expression [23]:

$$\bar{h}_{os} = 0.725 \left\{ \frac{\rho_f (\rho_f - \rho_v) g h_{fg} k_f^3}{\mu_f D_o (T_s - T_w)} \right\}^{0.25} \qquad (5)$$

The validity of the Reynolds number exponent 0.8 in equation (4) may be questionable for corrugated tubes due to the severity of the "roughness" in these enhanced tubes. An error in this exponent will influence the calculated values of C_i and $\bar{h}_{os}$. However, this exponent has been used by earlier investigations [7, 9, 10] with good success, and it was therefore assumed to be valid for the tubes tested during this study.

Table 2 gives ratios of the average Sieder-Tate coefficients for the enhanced tubes ($\bar{C}i_a$) to that of the smooth tube ($\bar{C}i_s$), and average outside heat transfer coefficients for the enhanced tubes ($\bar{h}o_a$) to that of the smooth tube ($\bar{h}o_s$) for each of the tube types. The ratios represent the mean values over the entire flow range of the cooling water. Maximum deviations around the mean are also listed.

It is evident that for all of the tubes, most of the enhancement occurs on the inside, with little increase or in some cases a decrease on the outside. This result agrees with the earlier findings of Young, Withers and Lampert [9], Catchpole and Drew [10] and Cunningham and Milne [11] who showed that, in general, most of the heat transfer improvement occurs on the cooling water side. Apparently, the flutes on the inside, in addition to increasing the heat transfer surface area, act as roughness elements to create additional turbulence. A swirl component of velocity is also generated which can give rise to secondary flows in the flute channels, effectively thinning the laminar sublayer, and increasing the heat transfer. All of these effects may contribute to the large increases as measured.

On the other hand, on the outside, the flutes generate surface tension driven forces which tend to thin the condensate film on the convex surfaces (ridges) and to thicken the film in the concave channels (valleys), as originally postulated by Gregorig [24] and recently described by Combs [13]. The thinner film on the ridges provides a lower thermal resistance to heat flow whereas the thicker film in the valleys provides a higher resistance. The overall heat transfer improvement depends upon a tradeoff between improvement on the ridges and degradation in the valleys. The greater amount of condensate in the valleys should provide for better drainage, but during these tests the condensate appeared to be held up on the flutes, presumably due to the high surface tension of water. Lower surface tension fluids, such as refrigerants, may therefore behave differently. In actual shell-side condensation, at high vapor velocities, shear forces at the liquid-vapor interface may rip the condensate off the tubes, effectively thinning the film and providing a heat transfer improvement on the outside.

Further study of Tables 1 and 2 shows that the inside and outside heat transfer coefficients are related to change in pitch for approximately constant groove depth. This is reflected in Fig. 9 which shows values of the ratios of $\bar{C}i_a/\bar{C}i_s$ and $\bar{h}o_a/\bar{h}o_s$ plotted versus varying pitch for constant groove depth. The trends of the data in the $\bar{C}i_a/\bar{C}i_s$ curve reveal that there is perhaps an optimum pitch, at a constant groove depth, which maximizes the inside heat transfer coefficient. This

Table 2. Summary of Internal and External Heat Transfer Coefficients of Enhanced Tubing

Tube No.	$\bar{C}i_a/\bar{C}i_s$	$\bar{h}o_a/\bar{h}o_s$
K-1	1.60 ± .18	.97 ± .11
K-2	2.12 ± .21	.93 ± .09
K-3	2.60 ± .47	.85 ± .09
K-4	2.60 ± .29	.85 ± .09
K-5	2.20 ± .27	1.15 ± .12
T-1	1.76 ± .24	1.03 ± .13
T-2	2.92 ± .33	1.10 ± .10
T-3a	4.88 ± .82	1.32 ± .12
T-3b	5.12 ± .90	1.34 ± .13
GA-1	3.28 ± .51	.94 ± .06
GA-2	3.24 ± .50	.94 ± .06
GA-3	3.28 ± .51	.99 ± .09

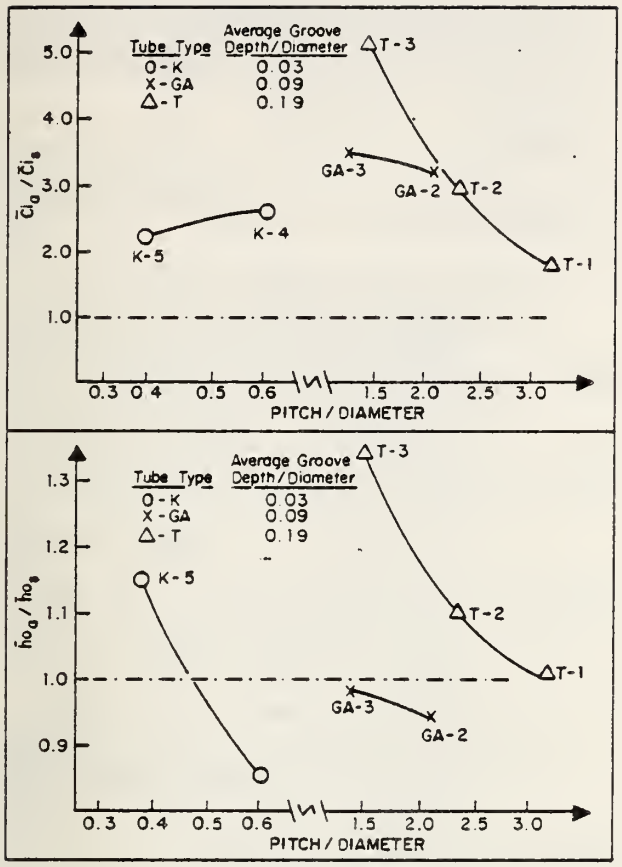

Fig. 9. Effect of Groove Depth and Pitch on Inside and Outside Heat Transfer Coefficients

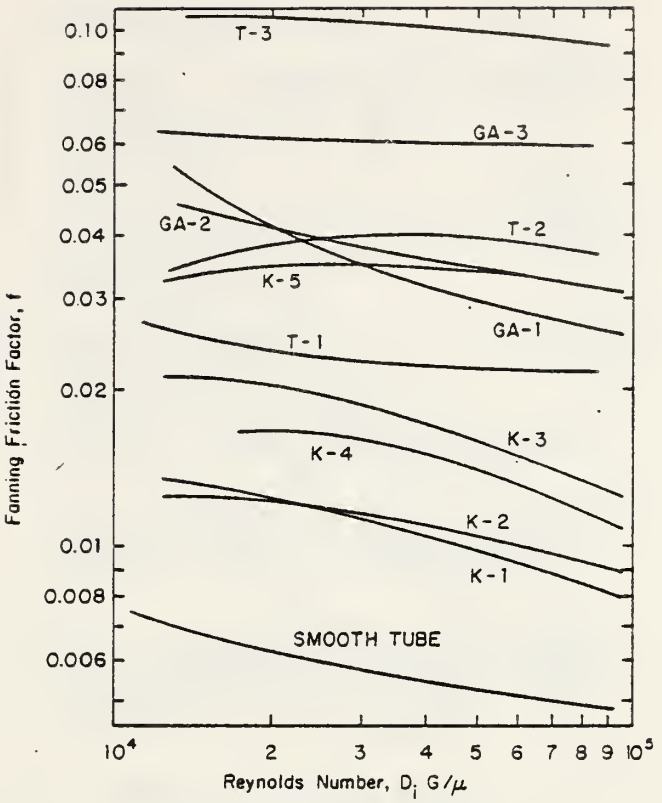

Fig. 10. Fanning Friction Factor for the Enhanced Tubes

could be due to the fact that as pitch changes from being very large to very small, the nature of the internal flow changes from predominately swirling motion to predominately turbulent mixing. The optimum pitch could therefore be the one that produces a combination of both these mechanisms. Figure 9 also shows outside heat transfer improves with decreased pitch. With reduced pitch, condensate drainage improves and more channels are provided, presenting more tube surface area to the steam flow. Notice that the relative position of the data for the three tube types is related to their respective groove depths. A deeper groove provides better heat transfer on both sides of the tube. These results correlate with the work of Catchpole and Drew [10]. In their results, for $e/D_o = 0.04$, decreasing p/D_o from about 0.8 to 0.4 increased the $\bar{C}i_a/\bar{C}i_s$ ratio from 2.1 to 2.6. This same decrease in pitch followed the trend of Figure 9 for the outside heat transfer coefficient, with a maximum $\bar{h}o_a/\bar{h}o_s$ ratio reached of about 1.7.

Friction Factor

Figure 10 shows the Fanning friction factors of the corrugated tubes. As expected, they are significantly higher than the smooth tube value. Tube T-3 shows the largest friction factor overall, and tubes K-5 and GA-3 show the largest friction factors for the other tube types. In examining the tube characteristics given in Table 1, it is apparent that as tube pitch decreases, or helix angle increases, the friction factor increases. As helix angle approaches 90°, the grooves appear as repeated rib-type roughness elements which have been studied by Webb, Eckert and Goldstein [25]. They show that as the height of the rib-roughness element (i.e., groove depth) increases, and as the distance between ribs decreases, (i.e., higher helix angle), the friction factors increase. These trends are clearly evident in Figure 10. Furthermore, it appears that the friction factors for tubes T-3, GA-3 and K-5 remain approximately independent of Reynolds number, indicating that the flow in these tubes is "fully rough."

Overall Tube Performance

Bergles [2] and Bergles, Blumenkrantz and Taborek [5] outline several performance criteria of enhanced tubes based on the inside heat transfer coefficients by solving for the ratio of augmented to smooth tube heat exchanger surface areas while holding various parameters constant. These criteria were later extended by Bergles, Bunn and Junkhan [6] to include external thermal resistances as well. A particular criterion of interest for condenser design is the ratio of augmented to smooth tube surface area for a given heat load, tube size, log mean temperature difference and pumping power. A smaller area ratio would require a shorter tube for the same performance. This criterion was therefore chosen to compare the overall performance of the corrugated tubes to one another. Details of this technique may be found in Fenner [17] and Reilly [18].

Figure 11 shows this area ratio for the corrugated tubes versus the Reynolds number in the smooth

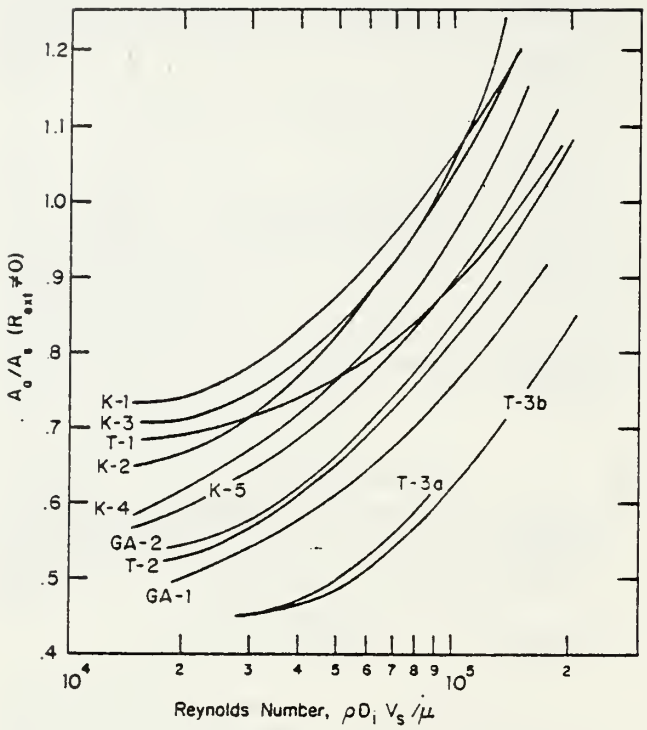

Fig. 11. Surface Area Ratio of Augmented Tube to Smooth Tube Condenser at Constant Heat Load and Pumping Power

tube. The figure is entered by picking a smooth tube velocity, and calculating a Reynolds number. For example, naval condensers are designed for a cooling water velocity of 2.74 m/s. Using this representative value in a 16 mm diameter smooth tube gives a smooth tube Reynolds number of about 40,000. The velocity and Reynolds number in the augmented tube would, of course, be less to preserve the same pumping power. Entering Figure 11 with this Reynolds number, it is seen that tube T-3 would allow for approximately a 33 percent reduction in the required surface area, whereas tube K-1 would allow for approximately a 17 percent reduction.

All of the tubes are more effective in reducing surface area at low rather than high smooth tube Reynolds numbers. This is because, in smooth tubes at low cooling water velocities (less than approximately 2.7 m/s), the tube-side thermal resistance is controlling. Since the corrugated tubes enhance heat transfer primarily on the inside, as shown earlier, then a significant reduction in surface area is possible for the same heat load and pumping power. At high Reynolds numbers, on the other hand, the steam-side thermal resistance is controlling and the corrugated tubes will not perform as well.

The results in Figure 11 should be interpreted with caution. The area ratios were calculated assuming the log mean temperature difference to be constant. In reality, during these tests the log mean temperature difference ranged between 35 and 46 C. This variation will shift the curves approximately 5 percent with respect to one another. More importantly, the results obtained don't take into account variations in tube diameter, or spacing, as well as steam flow and condensate inundation effects. Such parameters are extremely important in condenser design considerations, allowing the designer to adjust the frontal area as well as the length of the heat exchanger. Finally, the effects of fouling, tube vibration and cost may influence final tube choice.

CONCLUSIONS

As a result of the above-mentioned tests, the following conclusions are reached:

1. All of the corrugated tubes showed an improvement in the corrected overall heat transfer coefficient when compared to the smooth tube. This improvement ranged from 17 to 104 percent.
2. Most of this improvement occurred on the cooling water side of the tubes presumably due to a combination of increased surface area, as well as increased turbulence and induced swirl in the flow.
3. This increase in heat transfer occurred at the expense of a substantial increase in cooling water pressure drop. Measured friction factors were as much as ten times the smooth tube value.
4. Corrugated tubes manufactured with very deep grooves exhibited the best heat transfer performance. However, when these tubes were not properly supported, vibration occurred due to cooling water turbulence, which caused a deterioration in their performance.
5. At a constant groove depth, heat transfer performance was dependent upon groove pitch, or helix angle.
6. The use of these corrugated tubes in a surface condenser may reduce the required surface area by as much as 30 percent for a constant heat load and pumping power. The above result, however, doesn't include effects such as high steam velocity, condensate inundation in a tube bundle, and fouling, all of which may play an important role in condenser design.

REFERENCES

1. Bergles, A. E., "Enchancement of Heat Transfer," Proceedings of the Sixth International Heat Transfer Conference, Vol. 6, Toronto, 1978, pp. 89-108.

2. Bergles, A. E. and Jensen, M. K., "Enhanced Single-Phase Heat Transfer for Ocean Thermal Energy Conversion Systems". Research Report HTL-15, April 1977, Iowa State University, Ames, Iowa.

3. Bergles, A. E., "Bibliography on Augmentation of Convective Heat and Mass Transfer", Part 1, Previews of Heat and Mass Transfer, Vol. 4, No. 2, January 1978.

4. Bergles, A. E., "Bibliography on Augmentation of Convective Heat and Mass Transfer," Part 2, Previews of Heat and Mass Transfer, Vol. 4, No. 4, July 1978.

5. Bergles, A. E., Blumenkrantz, A. R., and Taborek, J., "Performance Evaluation Criteria for Enhanced Heat Transfer Surfaces," Proceedings of the Fifth International Heat Transfer Conference, Tokyo, 1974.

6. Bergles, A. E., Bunn, R. L., and Junkhan, G. H., "Extended Performance Evaluation Criteria for Enhanced Heat Transfer Surfaces," Letters in Heat and Mass Transfer, Vol. 1, 1974, pp. 113-120.

7. Palen, J., Cham, B. and Taborek, J., "Comparison of Condensation of Steam on Plain and Turbotec Spirally Grooved Tubes in a Baffled Shell-and-Tube Condenser", Report 2439-300/6, January 1971, Heat Transfer Research, Incorporated, Alhambra, California.

8. Palen, J., Cham, B. and Taborek, J., "Comparison of Condensation of Steam on Plain and Phelps Dodge Spirally Grooved Tubes in a Baffled Shell-and-Tube Condenser," Report 2430-300/5, December 1970, Heat Transfer Research, Incorporated, Alhambra. California.

9. Young, E. H., Withers, J. G. and Lampert, W. B., "Heat Transfer Characteristics of Corrugated Tubes in Steam Condensing Applications," AIChE Paper No. 3, 15th National Heat Transfer Conference, San Francisco, August 1975.

10. Catchpole, J. P. and Drew, B. C. H., "Evaluation of Some Shaped Tubes for Steam Condensers," Report No. 619, National Engineering Laboratory, East Kilbride, Glasgow, August 1976.

11. Cunningham, J. and Milne, H. K., "The Effect of Helix Angle on the Performance of Roped Tubes," Proceedings of the Sixth International Heat Transfer Conference, Vol. 2, Toronto, 1978, pp. 601-605.

12. Newson, I. H. and Hodgson, T. K., "The Development of Enhanced Heat Transfer Condenser Tubing," Proceedings of the Fourth International Symposium on Fresh Water From the Sea, Vol. 1, 1973, pp. 69-94.

13. Combs, S. K., "An Experimental Study of Heat Transfer Enhancement for Ammonia Condensing on Vertical Fluted Tubes," Report ORNL-5356, January 1978, Oak Ridge National Laboratory, Oak Ridge, Tennessee.

14. Combs, S. K., Mailen, G. S. and Murphy, R. W., "Condensation of Refrigerants on Vertical Fluted Tubes," ORNL/TM-5848, August 1978, Oak Ridge National Laboratory, Oak Ridge, Tennessee.

15. Beck, A. C., A Test Facility to Measure Heat Transfer Performance of Advanced Condenser Tubes, MSME, Naval Postgraduate School, Monterey, California, January 1977.

16. Pence, D. T., An Experimental Study of Steam Condensation on a Single Horizontal Tube, MSME, Naval Postgraduate School, Monterey, California, March 1978.

17. Fenner, J. H., An Experimental Comparison of Enhanced Heat Transfer Condenser Tubing, MSME, Naval Postgraduate School, Monterey, California, September 1978.

18. Reilly, D. J., An Experimental Investigation of Enhanced Heat Transfer on Horizontal Condenser Tubes, MSME, Naval Postgraduate School, Monterey, California, March 1978.

19. Metals Handbook, 8th ed., Vol 2, American Society for Metals, 1964, p. 665.

20. Wilson, E. E., A Basis for Rational Design of Heat Transfer Apparatus, paper presented at the Spring Meeting of the Society of Mechanical Engineers, Buffalo, N.Y., June 1935.

21. Briggs, D. E., and Young, E. H., "Modified Wilson Plot Techniques for Obtaining Heat Transfer Correlations for Shell and Tube Heat Exchangers," Heat Transfer-Philadelphia, Vol. 65, No. 92, 1969, pp. 35-45,

22. Sieder, E. N., and Tate, C. E., "Heat Transfer and Pressure Drop of Liquids in Tubes," Ind. Eng. Chemistry, Vol. 28, 1936, p. 1429.

23. Holman, J. P., Heat Transfer, 4th Ed., McGraw-Hill Book Co., New York, 1976, p. 358.

24. Gregorig, R., "Film Condensation on Finely Waved Surfaces with Consideration of Surface Tension," Zeit. Fur Ang. Math. U. Physik, Vol. 5, 1954, p. 36.

25. Webb, R. L., Eckert, E. R. G., and Goldstein, R. J., "Heat Transfer and Friction in Tubes with Repeated-Rib Roughness," Int. J. of Heat Mass Transfer, Vol. 14, 1971, pp. 601-617.

APPENDIX B: Some Comments on Rain Effects

Nomenclature:

g	acceleration of gravity
$\bar{h}_{cn}$	average heat transfer coefficient for n tubes
h_n	heat transfer coefficient for the n-th tube
h_N	heat transfer coefficient for a single tube
n	number of tubes
k_f	condensate film thermal conductivity
ΔT_f	temperature drop across condensate film
ρ	density of condensate film
ρ_v	density of vapor
μ_f	viscosity of condensate film

Nusselt Model:

If each tube in a column of n tubes condenses at the same rate and if the condensate from each tube is added to the film of the tube below in such a way that the assumptions of the single-tube analysis remain valid, then the average film coefficient for a row of n tubes is

$$\bar{h}_{cn} = 0.728 \left[\frac{g\rho(\rho - \rho_v)k_f^3 h_{fg}}{n\mu_v \Delta T_f}\right]^{\frac{1}{4}}$$

If h_N is the film coefficient for a single tube ($n = 1$ in the above expression) then

$$\frac{\bar{h}_{cn}}{h_N} = n^{-0.25} \qquad (1)$$

From an expression such as (1), we may find simple formulas for the individual tubes in the column. Thus, from the definition of the mean,

$$\bar{h}_{cn} = \frac{1}{n} \sum_{i=1}^{n} h_i, \text{ and } \bar{h}_{c(n-1)} = \frac{1}{n-1} \sum_{i=1}^{n-1} h_i$$

so that

$$n\bar{h}_{cn} - (n-1)\bar{h}_{c(n-1)} = \sum_{i=1}^{n} h_i - \sum_{i=1}^{n-1} h_i = h_n$$

and applying (1) separately for n and (n-1) tubes

$$h_n = nh_N (n)^{-.25} - (n-1) h_N (n-1)^{-.25}$$

or

$$\frac{h_n}{h_N} = n^{.75} - (n - 1)^{.75} \qquad (2)$$

Equation (2) is plotted below for a range of values of n. Note that the Nusselt result indicates that any tubes over about 5 give less than 50% performance. In fact, experimental results of various investigators show that Eq. (1) is more appropriately written

$$\frac{\bar{h}_{cn}}{h_n} = n^{-s}$$

where s may vary in the range of 0.07 to 0.20. Results using the extreme value (s = 0.07) are also plotted below. Note that in this case over 1000 tubes are required before tube performance is degraded below 50%. Clearly there are large

discrepancies in the Nusselt model for multiple-tube effects.

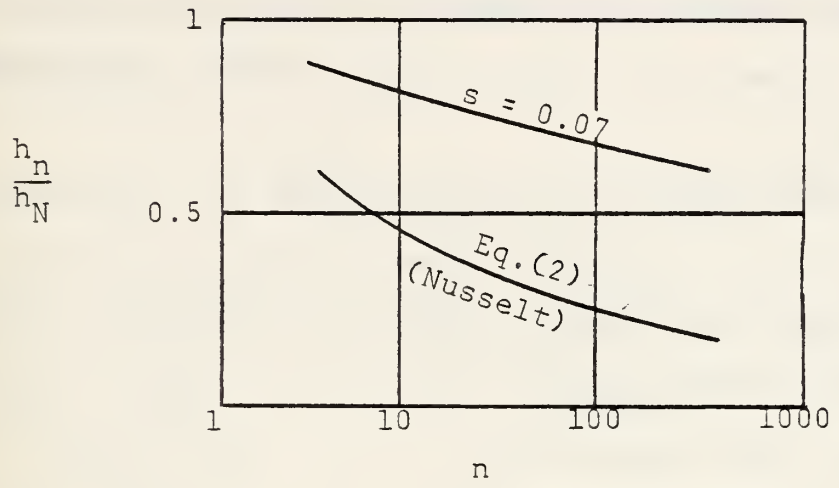

There are a variety of effects that are not accounted for in the Nusselt multiple-tube prediction. These include:

1. Multiple-tube spacing and orientation.
2. Condensate momentum. The location and nature of the separation of the condensate film are variable: Trajectories of condensate drops and rivulets will vary accordingly.
3. Vapor shear. This can drastically affect the form of the condensate film and the nature of the condensate separation. In addition, the liquid particles will be convected by the vapor flow during their journies between tubes.

The Eissenberg Side-Drainage Model:

Eissenberg[1] has proposed a model of condensate drainage that tends to evaluate the limits of the effect in the absence of vapor shear.

It is hypothesized that, in the extreme, all condensate from a given tube in a staggered array flows to one or the other of the next-lower tubes in the adjacent columns. With perfect symmetry, this process should alternate back and forth as a droplet of condensate proceeds down the bundle (dotted line in the sketch). In such a pattern, tube 3 will receive condensate from tubes 1 and 2, tube 5 will be fed by tubes 1, 2, 3, and 4, etc. Each tube will receive twice the condensate that it would have received from drainage in a strictly vertical (tube bottom-tube top) pattern such as that given by the Nusselt theory.

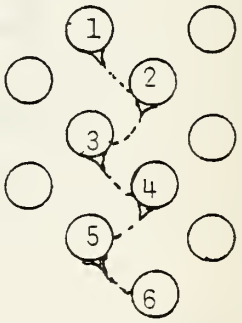

If the drainage condensate affected the entire area of each tube, the Nusselt model could be modified by simply replacing n by 2n. Eissenberg suggests, however, that the drainage influence is confined to the lower regions of each tube so that, in general, the above assumption (n → 2n) would

---

[1]Eissenberg, D. M., Investigation of the Variables Affecting Steam Condensation on the Outside of Tube Bundles, Ph.D. diss., U. Tenn., Dec. 1972.

over-predict the effect. The assumption is made that only the lower half of each tube receives drainage liquid from tubes above. Thus

$$\frac{\bar{h}_{cn}}{h_{N\ (\text{tube bottoms})}} = \frac{1}{2}(2n)^{-.25}$$

With no condensate drainage, the Nusselt model indicates that the top halves of tubes carry 60% of the condensing load so that

$$\frac{\bar{h}_{cn}}{h_N}\ (\text{tube tops}) = 0.6$$

Eissenberg postulates that with total side-drainage, the reduction in h_N is given by the sum of these expressions:

$$\frac{\bar{h}_{cn}}{h_N} = 0.6 + \frac{1}{2}(2n)^{-.25} \qquad (1)$$

If there is a flow pattern that lies between the Nusselt and the total side-drainage cases, a linear weighting may be used without further restricting the analysis:

$$\frac{\bar{h}_{cn}}{h_N} = (1 - F_d)n^{-.25} + F_d\left[0.6 + \frac{1}{2}(2n)^{-.25}\right] \qquad (2)$$

or

$$\frac{\bar{h}_{cn}}{h_N} = 0.6\ F_d + \frac{1 - 0.58\ F_d}{n^{.25}}$$

Here F_d is the "drainage factor" and varies from 1 for total side drainage to 0 for Nusselt drainage (tubes in line and/or widely spaced).

Figure B1 is offered by Eissenberg in support of his theory. Since the value of s = 0.25 is somewhat disproven, calculations have also been made with a value of s based upon the data of Ferguson and Oakden (as presented by Eissenberg) for the column case (where Nusselt's approximations might be expected to have some validity). This lead to s $\simeq$ 0.20 so that

$$\frac{\bar{h}_{cn}}{h_N} = (1 - F_d)n^{-0.2} + F_d \left[0.6 + \frac{1}{2}(2n)^{-0.2}\right] \qquad (2a)$$

The points (X) on the figure mark results using this equation with F_d = 1 and with F_d = 0. The agreement of Eq. (2a) with the data in Fig. A1 is remarkable. This indicates promise for future work to relate the value of s to condenser design variables.

It is reemphasized that the theory given above does not take vapor shear effects into account. It may, however, be a valid basis upon which we can develop a theory that can be extended to apply to tube bundles under a shear-dominated flow condition.

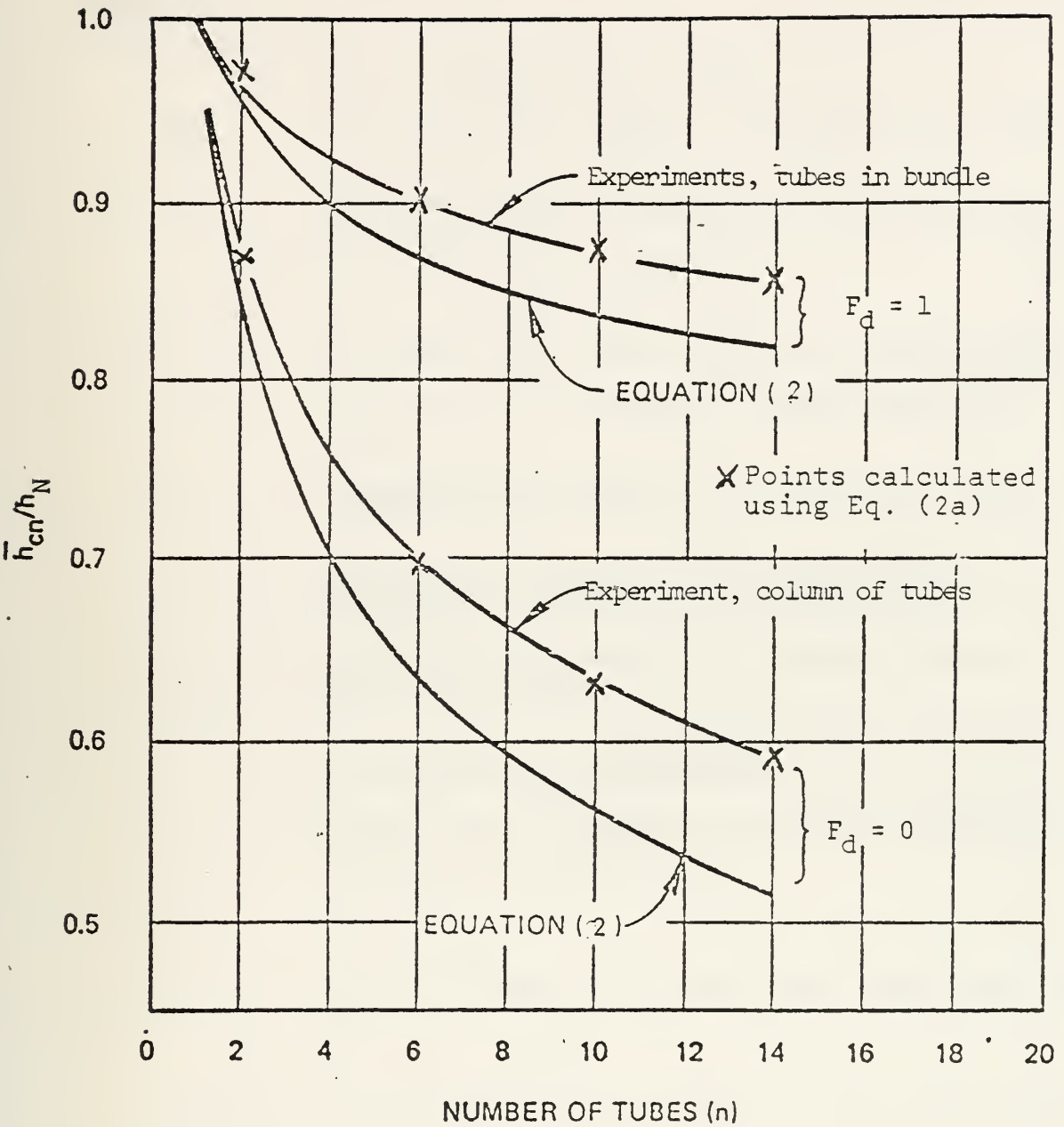

Figure B1. Comparison of data of Ferguson and Oakden with analytical expressions.

APPENDIX C: Noncondensible Gas Effects

Nomenclature:

A	heat transfer surface area
h_{eff}	effective heat transfer coefficient for non-condensible gas film
h_g	film heat transfer coefficient for sensible heat transfer
k_g	mass transfer coefficient
m	condensate mass flow rate for a single tube
P_{sb}	steam partial pressure at bulk conditions (T_{sat})
P_{sc}	steam partial pressure at condensate film surface (T_c)
T_c	saturation temperature at steam partial pressure at condensate film surface
T_{sat}	saturation temperature at external steam partial pressure
U	overall heat transfer coefficient excluding noncondensible gas effects
U_g	overall heat transfer coefficient including noncondensible gas
ΔT_g	$T_{sat} - T_c$
ΔT_m	log-mean temperature difference associated with U_g

Because of the condensation of steam at the tube surface the proportion of steam in a steam-gas mixture decreases near the tube surface: the steam partial pressure decreases across the gas film. This gradient of partial pressure results in mass transfer of steam across the gas film at a rate equal to

the rate of condensation. The mass transfer coefficient is defined as

$$k_g = \frac{m/A}{(P_{sb} - P_{sc})}$$

An energy balance across the gas film gives:

$$h_{eff}(T_{sat} - T_c) = h_{fg}\, k_g(P_{sb} - P_{sc}) + h_g(T_{sat} - T_c)$$

The sensible heat transfer term is usually neglected (about 0.1% or less) so that

$$h_{eff} \simeq h_{fg} k_g \frac{(P_{sb} - P_{sc})}{(T_{sat} - T_c)} \qquad (1)$$

In ORCON, the value of h_{eff} is calculated as follows:

$$h_{eff}\, \Delta T_g = U_g\, \Delta T_m \qquad (2)$$

where U_g is the overall film coefficient <u>with</u> the n.c. film such that

$$\frac{1}{U_g} = \frac{1}{U} + \frac{1}{h_{eff}} \qquad (3)$$

U is the overall film coefficient without the n.c. film and is known from the previous calculations.

Eliminating h_{eff} from (2) and (3)

$$U\Delta T_m = U_g \Delta T_g \qquad (4)$$

and from (1)

$$\Delta T_g = T_{sat} - T_c = \frac{k_g h_{fg}(P_{sb} - P_{sc})}{h_{eff}} = k_g h_{fg} \Delta P_g \left(\frac{1}{U_g} - \frac{1}{U}\right)$$

which, when combined with (4) yields a quadratic in U_g:

$$U_g^2 - UU_g + \frac{k_g h_{fg}}{\Delta T_m} \Delta P_g (U - U_g) = 0 \qquad (5)$$

ΔP_g is eliminated by defining the term:

$$j_m = \frac{k_g P_{gc} (Sc)^{2/3}}{G_v}$$

where Sc is the Schmidt number and G_v is the mass velocity of the vapor-gas mixture.

The result is:

$$U_g^2 - \left[U + \frac{h_{fg} j_m G_v S_c^{-2/3}}{\Delta T_m} + \frac{U P_{gb}}{\Delta T_m} \left(\frac{\Delta T_g}{\Delta P_g}\right)\right] U_g + \frac{U h_{fg} j_m G_v S_c^{-2/3}}{\Delta T_m} = 0$$

U is the uncorrected (single component) overall film coefficient. P_{gb} is the partial pressure of the noncondensibles at the given steam temperature. Both j_m and $(\Delta T_g / \Delta P_g)$ are evaluated from empirical data. With U_g calculated from the above, h_{eff} is found from Eq. (3).

APPENDIX D: Initial Trajectory of a Condensate Droplet

We seek to estimate the initial trajectory of a spherical droplet of diameter d that is imagined to have its origin in the condensate film prior to falling into a vapor stream. The following analysis is approximate and only those simplifications that are not obvious will receive comment. In the sketches, the droplet is shown in the fixed coordinate system with its initial position of (0,0).

The steam velocity U_s is in the x - direction and is initially the velocity relative to the droplet. The statement of dynamic equilibrium of the droplet is

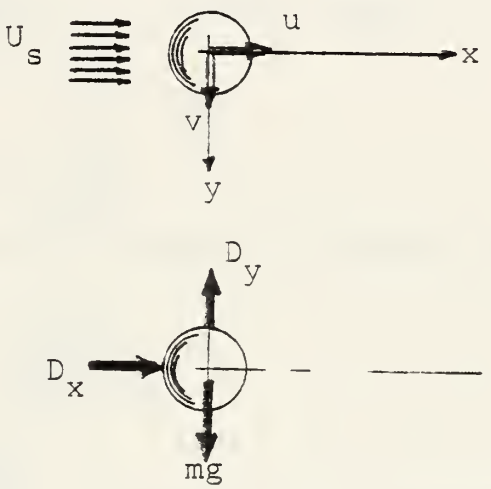

$$\Sigma F_x = m\frac{du}{dt}$$

$$\Sigma F_y = m\frac{dv}{dt}$$

and in the x and y directions, respectively we consider the forces of gravity and aerodynamic drag:

$$\Sigma F_x = D_x$$

$$\Sigma F_y = mg - D_y$$

Solution in the direction of steam flow:

For the x - direction we have:

$$m\frac{du}{dt} = \bar{C}_{Dx}\frac{1}{2}\rho_s(U_s - u)^2 A \qquad (1)$$

where $(U_s - u)$ is the velocity of steam relative to the droplet in the x-direction and $\bar{C}_{Dx}$ is an average drag coefficient taken to be constant over the range of velocities occuring in the time increment of calculation (more on this later).

If we define non-dimensional quantities $\hat{u}$, $\hat{C}_{Dx}$, and τ such that

$$\tau = \frac{tU_s}{d}, \quad \hat{u} = \frac{u}{U_s}, \quad \hat{C}_{Dx} = \frac{3}{4}\bar{C}_{Dx}\left(\frac{\rho_s}{\rho}\right) \tag{2}$$

(ρ_s = steam density, ρ = condensate density) then

$$\frac{d\hat{u}}{d\tau} = \hat{C}_{Dx}(1 - \hat{u})^2 \tag{3}$$

the solution of which, with $\hat{u}(0) = 0$, is

$$\hat{u} = \frac{\hat{C}_{Dx}\tau}{1 + \hat{C}_{Dx}\tau} \tag{4}$$

Defining $\hat{x} = \frac{x}{d}$, then $\hat{u} = \frac{d\hat{x}}{d\tau}$, and Eq. (4) is again integrated ($\hat{x}(0) = 0$)

$$\hat{x} = \tau - \frac{1}{\hat{C}_{Dx}} \ell n(1 + \hat{C}_{Dx}\tau) \tag{5}$$

Solution in the direction of gravity:

For the y - direction we have

$$m\frac{dv}{dt} = mg - \bar{C}_{Dy}\left(\frac{1}{2}\rho_s v^2\right)A \tag{6}$$

In this case we need not assume a constant mean value for $\bar{C}_{Dy}$ since v(0) = 0 and slow flow is a reasonable assumption, that is

$$\bar{C}_{Dy} = \frac{24}{Re} = \frac{24}{\frac{vd}{\nu_s}}$$

(beyond the slow-flow region, the problem can be solved in the y-direction in a way that follows the method used for the x-direction.) Equation (6) may now be written:

$$m\frac{dv}{dt} = mg - 12(\rho_s \upsilon_s dA)v$$

With

$$\hat{v} = \frac{v}{U_s} \quad \text{and} \quad Fn = \frac{U_s}{\sqrt{gd}}$$

$$\frac{d\hat{v}}{d\tau} = \frac{1}{Fn^2} - \frac{18}{Re_s}\left(\frac{\rho_s}{\rho}\right)\hat{v}$$

where

$$Re_s = \frac{U_s d}{\upsilon_s}$$

Defining a modified Reynolds number:

$$Re_p = \frac{U_s d}{\upsilon_s}\left(\frac{\rho}{\rho_s}\right) = \frac{\rho U_s d}{\mu_s}$$

we have

$$\frac{d\hat{v}}{d\tau} = \frac{1}{Fn^2} - \frac{18}{Re_p}\hat{v} \qquad (7)$$

Upon integration with $\hat{v}(0) = \hat{y}(0) = 0$, we have

$$\hat{v} = \frac{Re_p}{18Fn^2}\left(1 - e^{-\frac{18\tau}{Re_p}}\right) \tag{8}$$

and

$$\hat{y} = \frac{y}{d} = \frac{Re_p}{18Fn^2}\,\tau - \frac{Re_p}{18}\left(1 - e^{-\frac{18\tau}{Re_p}}\right) \tag{9}$$

Initial Trajectory:

If Eqs. (8) and (9) are expanded in series form, we have

$$\hat{v} = \frac{\tau}{Fn^2}\left[1 - \tfrac{1}{2}\left(\frac{18\tau}{Re_p}\right) + \frac{1}{3!}\left(\frac{18\tau}{Re_p}\right)^2 - \ldots\right]$$

$$\hat{y} = \tfrac{1}{2}\frac{\tau^2}{Fn^2}\left[1 - \frac{2}{3!}\left(\frac{18\tau}{Re_p}\right) + \frac{2}{4!}\left(\frac{18\tau}{Re_p}\right)^2 - \ldots\right]$$

and for sufficiently small values of $\frac{18\tau}{Re_p}$ the initial terms become gravity dominated because shear in the vertical direction does not act until a vertical velocity is developed. Our expressions for small τ are:

$$\hat{v}_i = \frac{\tau}{Fn^2} \tag{8i}$$

$$\hat{y}_i = \frac{1}{2}\left(\frac{\tau}{Fn}\right)^2 \tag{9i}$$

The initial trajectory may be estimated by eliminating τ from Eqs. (5) and (9i) with the result:

$$\hat{x}_i = \sqrt{2}\, Fn\, \hat{y}_i^{\frac{1}{2}} - \frac{1}{\hat{C}_{Dx}} \ell n(1 + 2\, Fn\, \hat{C}_{Dx} \hat{y}_i^{\frac{1}{2}}) \qquad (10)$$

Criterion for gravity dominance:

If we define $\theta_i = \tan^{-1} \frac{v_i}{u}$, we have from Eqs. (4) and (8i)

$$\theta_i = \tan^{-1} \frac{1}{\hat{C}_{Dx} Fn^2} \qquad (11)$$

subject to the condition $\hat{C}_{Dx}\tau << 1$. From a trajectory point of view the flow may be considered to be gravity dominated for cases in which θ_i is greater than some specified value. The value specified should depend upon the layout of the tube bundle but for generality here we select 45^o as a point of demarcation. That is

$$\theta_i > 45^o \rightarrow \text{gravity dominance}$$

which gives, from Eq. (11)

$$\hat{C}_{Dx} Fn^2 < 1 \rightarrow \text{gravity dominance} \qquad (12)$$

Sample calculations: The foregoing analysis requires that the value of $\bar{C}_{Dx}$ remain approximately constant during the calculation period. This condition can be achieved if the drag in the x-direction is mainly form drag or, in other words, if

$$10^3 < Re_s < 10^5$$

in which case $\bar{C}_{Dx} \simeq 0.4$ for a spherical particle. For our sample calculations we shall select the following rough values:

droplet diameter: $d = \frac{1}{4}$ inch

steam properties: $\upsilon_s \simeq 1.2 \times 10^{-3}$ ft^2/sec

$\rho_s \simeq 1.75 \times 10^{-4}$ lb sec^2/ft^4

$\mu_s \simeq 2.1 \times 10^{-7}$ lb sec/ft^2

The criterion for constant $\bar{C}_{Dx}$ then becomes, approximately,

$$60 < U_s < 6000 \text{ ft/sec}$$

which is a reasonable range of calculation for condenser conditions. For water droplets, $\rho_s/\rho \simeq 10^{-4}$ and therefore

$$\hat{C}_{Dx} = \frac{3}{4} \bar{C}_{Dx} \left(\frac{\rho_s}{\rho}\right) = 3 \times 10^{-5}$$

Recall that a criterion for validity of this approach is $\hat{C}_{Dx} \tau << 1$ or now, $\tau << 3 \times 10^4$. In dimensional terms $tU_s/d << 3 \times 10^4$, a criterion that is easily satisfied except for unrealistically high steam speeds. The criterion (12) may be written in terms of a critical steam speed below which the droplet trajectory will be gravity dominated:

$$\left(\hat{C}_{Dx} F_n^2\right)_{crit} = 1$$

or

$$\left[\frac{3}{4} \bar{C}_{Dx} \left(\frac{\rho_s}{\rho}\right)\left(\frac{U_s^2}{gd}\right)\right]_{crit} = 1$$

With the above constant values for $\bar{C}_{Dx}$ and the density ratio we have

$$\left(\frac{U_s^2}{d}\right)_{crit} = 1.073 \times 10^{-6}$$

With U_s in ft/sec and d in ft. This expression is plotted below.

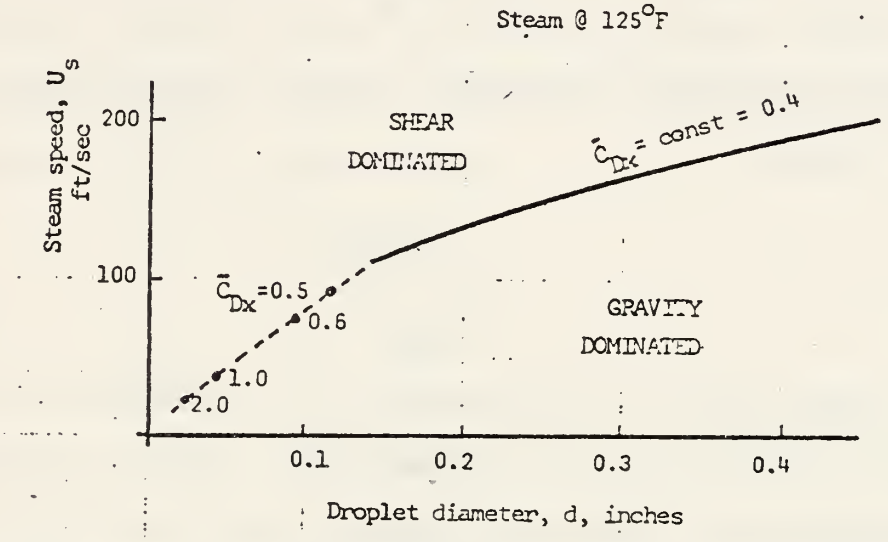

These are sample calculations only and serve to illustrate the kinds of logic that can be developed from the analysis. The most important result is that the parameter

$$N = \hat{C}_{Dx} Fn^2 = \frac{3}{4} \bar{C}_{Dx} \left(\frac{\rho_s}{\rho}\right)\left(\frac{U_s^2}{gd}\right)$$

is a measure of the relative influence of shear and gravity upon the initial droplet trajectory. Semi-empirical values of $\bar{C}_{Dx}$ in this expression will further specify the region of dominance.

Droplet residence times. A number of other interesting results can be obtained from the analysis outlined above. An example is the estimation of transport times applicable to

condenser bundles. From Eq. (4) the time required for a droplet to reach one-half of the speed of the steam is given by $\hat{u} = \frac{1}{2}$ and

$$\tau_{\frac{1}{2}} = \frac{1}{\hat{C}_{Dx}} = \frac{t_{\frac{1}{2}} U_s}{d}$$

Using the previously estimated vlaue of $\hat{C}_{Dx}$ we have, for a $\frac{1}{4}$-inch droplet

$$t_{\frac{1}{2}} = \frac{694}{U_s}$$

which gives values in the range of 5 - 15 seconds for steam speeds of 150-50 ft/sec, respectively. Naval condensers have steam paths that are, typically, on the order of 5 ft. long. The time for a $\frac{1}{4}$-inch particle to traverse such a distance (in the absence of other tubes or obstructions) may be estimated from Eq. (5) by finding the value τ corresponding $\hat{x} = 5(48) = 240$. The result is, approximately, $\tau_t = 87.5/U_s$. For U_s in the range of 50 - 150 ft/sec this gives droplet traverse times in the order of 1.75 - .6 seconds. The corresponding droplet speeds at the condenser exit are 5.6 - 16.8 ft/sec. Thus the inertia of the droplets causes them to lag well behind the vapor. A significant implication of this result is that condensate droplets tend to "see" a relative velocity equal to that of the surrounding vapor and that acceleration of the droplets by the drag of the vapor does not

lead to large changes in relative velocity - the droplets do not come anywhere near terminal velocity in the shear direction while they are inside of the condenser bundle. This conclusion lends support to the approximation of constant drag coefficient. In addition, the constraint of $C_{Dx}\,\tau << 1$ is largely met for droplet motion within all but the largest tube bundles. From the results, the following approximate forms should be valid in most cases:

$$\hat{u} \simeq C_{Dx}\,\tau$$

$$\hat{x} \simeq \frac{C_{Dx}}{2}\,\tau^2$$

$$\hat{v} \simeq \frac{\tau}{Fn^2}$$

$$\hat{y} \simeq \tfrac{1}{2}\left(\frac{\tau}{Fn}\right)^2$$

and

$$\frac{\hat{v}}{\hat{x}} \quad \frac{1}{\hat{C}_{Dx}Fn^2} = \tan\theta$$